UNIVERSITY OF TARTU

Faculty of Science and Technology

Institute of Chemistry

Verner Sääsk

Preparation of Luminescent Ionic Liquids Based on an Anionic Platinum(II) Complexes for Application in Optoelectronic Devices

Bachelor's thesis in Chemistry (6 ECTS)

Supervisors: Masaki Yoshida, PhD

Kaija Põhako-Esko, PhD

Vladislav Ivaništšev, PhD

Tartu 2021

ABSTRACT

Preparation of Luminescent Ionic Liquids Based on an Anionic Platinum(II) Complexes for Application in Optoelectronic Devices

This study reports on the successful preparation of four luminescent ionic liquids, for which melting temperatures, luminescence spectra, emission lifetime, and absolute quantum yield were measured. Based on measurement results, $[P_{6,6,6,14}][Pt(PPy)Cl_2]$ ($P_{6,6,6,14}$ = trihexyltetradecylphosphonium ion; PPy = 2-phenylpyridine) was chosen for closer investigation as most prominent of prepared materials, due to its remarkable quantum yield (at room temperature $\Phi = 0.40$) and low melting point ($T_m = 50$ °C). It was then demonstrated, that $[P_{6,6,6,14}][Pt(PPy)Cl_2]$ has all required properties to be applied in various optoelectronic devices, such as temperature sensors and displays based on organic light-emitting diodes or electrochemical cells.

CERCS: P360 Inorganic chemistry; P395 Organometallic chemistry; P402 Photochemistry.

Keywords: ionic liquids, platinum complexes, inorganic chemistry, quantum yield, optoelectronics, organic light-emitting diode.

INFOLEHT

Anioonsetel plaatina(II) kompleksidel põhinevate luminestsentsete ioonsete vedelike valmistamine optoelektroonilisteks rakendusteks

Käesolevas töös valmistati neli luminestsentset ioonset vedelikku ning mõõdeti nende sulamistemperatuurid, luminestsentsspektrid, emissiooni eluajad ja absoluutsed kvantsaagised. Mõõtmistulemuste põhjal valiti edasisteks uuringuteks ühend $[P_{6,6,6,14}][Pt(PPy)Cl_2]$ ($P_{6,6,6,14}$ = triheksüültetradetsüülfosfooniumioon; PPy = 2-fenüülpüridiin), tema väljapaistva kvantsaagise (toatemperatuuril Φ = 0,40) ja madala sulamistemperatuuri (T_m = 50 °C) tõttu. Seejärel demonstreeriti, et ühendil $[P_{6,6,6,14}][Pt(PPy)Cl_2]$ on kõik vajalikud omadused, et seda saaks kasutada optoelektrooniliste seadmete, sealhulgas termosensorite ja orgaanilistel valgusdioodidel põhinevate ekraanide valmistamiseks.

CERCS: P360 Anorgaaniline keemia; P395 Organometalliline keemia; P402 Fotokeemia.

Märksõnad: ioonsed vedelikud, plaatina kompleksid, anorgaaniline keemia, kvantsaagis, optoelektroonika, orgaaniline valgusdiood.

CONTENTS

LIST OF ABBREVIATIONS USED

$[BMIm]^+$	1-butyl-3-methylimidazolium ion
$[P_{6,6,6,14}]^+$	trihexyltetradecylphosphonium ion
$[TBA]^+$	tetrabutylammonium ion
Cat	cation
DCM	dichloromethane
DMSO	dimethyl sulfoxide
DSC	differential scanning calorimetry
DTA	differential thermal analysis
Eq	equivalent
EtOH	ethanol
Hal	halide ion
IL	ionic liquid
LED	light-emitting diode
LEEC	light-emitting electrochemical cell
LIL	luminescent ionic liquid
MHz	megahertz
NA	not available
NMR	nuclear magnetic resonance
OLED	organic light-emitting diode
ppm	parts per million
PPy	2-phenylpyridine
RT	room temperature
TG	thermogravimetric
UV	ultraviolet

INTRODUCTION

The first two decades of the 21st century will probably be remembered for a remarkable development of optoelectronic devices, such as photochromic sensors [1,2], light-emitting electrochemical cells (LEECs) [3,4], and light-emitting diode (LED) displays [5].

Lately, the development of flexible displays had emerged as an economically crucial trend, supported by many major electronic companies, such as LG, Samsung, and Apple [6,7]. Among numerous other display technologies, LEECs and organic light-emitting diodes (OLEDs) are being used most often to produce flexible displays for the new generation of rollable TVs and foldable smartphones [3,5,8,9]. The key role of those thin luminescent film based technologies in the development and production of innovative displays is highlighted by the increase in the number of patents and investments into this field during the last ten years [7]. Furthermore, experts predict even larger funding flow into the LEEC and OLED development in the nearest future [4,5,7].

Despite the remarkable success of OLED and LEEC technologies, there are yet some challenging tasks in the field remaining. Currently, major issues are low quantum efficiency, narrow electrochemical window, and limited operation lifetime of the emitters in those systems [6–8]. To address those problems, researchers have turned their attention to a possible application of ionic liquids (ILs) as emitters in OLEDs and LEECs [10–13]. ILs are well-known for their wide electrochemical window and thermal stability [13], but a preparation of luminescent ionic liquids (LILs) with a high quantum yield is still a challenging issue [11]. Most recent research in this field focuses on using transition and rare-earth metal complexes as a luminescence centers for LILs [10,11,13–16].

During the last decade, transition and rare-earth metal-based materials have also found wide application in photochromic sensors, especially in the development of luminescent thermometers [1]. Luminescent thermometers had attracted much attention due to their high sensitivity and self-calibrating ability [17–21]. They are also potentially applicable in nanoscale systems, where traditional liquid-filled or bimetallic thermometers are not suitable [22].

Motivated by the emerging fields of flexible displays and photochromic sensors, this study focuses on developing LILs based on anionic platinum(II) complexes for their potential use as an emitter material in OLED and LEEC systems and photochromic sensors. This work aims to prepare LILs with an absolute quantum yield of at least 0.20 at room temperature.

1 LITERATURE OVERVIEW

1.1 Luminescence

Luminescence is an emission of photons by a molecule, occurring when an excited electron returns to its ground state. Luminescence can be divided into categories based on the mechanism of electron excitation, such as bioluminescence, electroluminescence, thermoluminescence, or photoluminescence. Photoluminescence is usually divided into fluorescence and phosphorescence, based on the nature of relaxation processes [23]. Fluorescence is characterized by the direct relaxation of an electron from an excited state (S_1) to the ground state (S_0), which is a relatively fast process taking about 10^{-12} seconds or less to happen [24]. In addition, an electron transition from a singlet excited state to an energetically favorable triplet excited state (T_1) is sometimes possible. This transition is called intersystem crossing, and it gives rise to a phosphorescence phenomenon (see Figure 1) [25]. Even though intersystem crossing is an almost instant process, the transition from triplet excited state back to the ground state is noticeably slower, taking about 10^{-6} to 10^{2} seconds [24]. This time delay makes phosphorescent materials glow for a longer time after excitation, in the case of some materials for days or even longer [25]. This phenomenon is widely known as an afterglow.

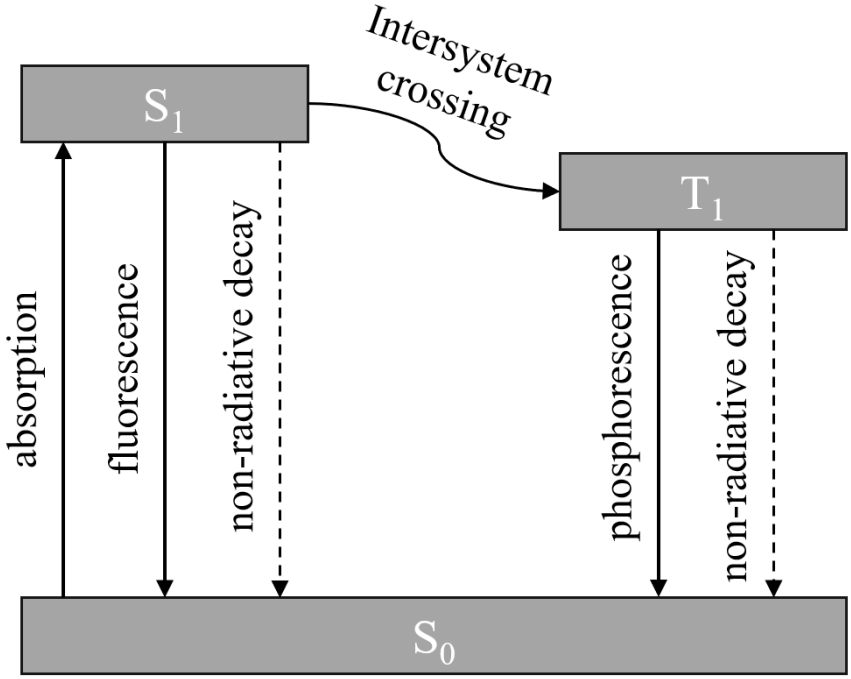

Figure 1. Schematic diagram showing the difference between fluorescence and phosphorescence.

Fluorescence and phosphorescence are usually called radiative decay processes because photons are emitted when excited electrons relax via fluorescence or phosphorescence [26].

Non-radiative decay processes, which arise from vibrational relaxation, are also possible (see Figure 1). Non-radiative decay is strongly correlated with temperature and becomes important at ~250 K [25].

1.2 Luminescence spectroscopy

Luminescence techniques, such as fluorescence spectroscopy and fluorescence lifetime measurements, are prominent analytical and detection tools used in contemporary science [27]. Luminescence techniques are non-invasive, suitable for remote sensing, and relatively easy to use; luminescence detection techniques are so sensitive that they can detect a single luminescent molecule [27]. Non-invasiveness and sensitivity make luminescence techniques a perfect bioimaging tool. They are also used for multiple other systems, such as metal-ligand complexes, polymeric nanoparticles, organic dyes, *etc*. [24].

To characterize luminescence properties of a material, emission and excitation spectra, as well as emission lifetime and quantum yield, are usually measured [25]. Emission spectra are useful in describing the emission color and intensity of a material luminescence, while excitation spectra are needed to determine absorption maxima. By measuring emission lifetime, one can understand the nature of emission, revealing insights on mechanisms of electron relaxation. Quantum yield measurement is required to describe the luminescence intensity.

1.2.1 Luminescence spectra

Typical measurement of luminescence spectra consists of two parts: measuring emission spectra and then excitation spectra [28]. For emission spectra, first, a certain excitation wavelength is chosen. Next, the remaining light from the light source is screened out via monochromator. Then the sample is irradiated at chosen wavelength, and emitted light is registered with the detector. By varying different excitation wavelengths, absolute emission maximum as well as the general shape of emission can be determined [28].

Excitation spectra measurement starts with choosing a desired emission wavelength, commonly the one corresponding to emission maximum [29]. Spectrum is then obtained by varying the wavelength of light passing through the excitation monochromator [29]. The excitation spectrum gives insights into the electron distribution of the molecule in the ground state, showing at which wavelength the sample is absorbing photons [28]. Therefore, excitation spectra can be compared to the absorption spectra [29].

It is essential to mention that photons emitted by the sample will generally have a longer wavelength than the photons absorbed by the sample [25]. This phenomenon is called Stokes shift, and it was first discovered by the pioneer of luminescence research, Sir George Gabriel Stokes, in 1852 [23]. Stokes shift is explained by the non-radiative decay processes, which happen at an excited state and decrease energy of electron [26]. When electrons eventually return to the ground state via luminescence and emit photons, the energies of the emitted photons are no longer equal to the energy of absorbed photons, resulting in certain shift between excitation and emission spectra (see Figure 2).

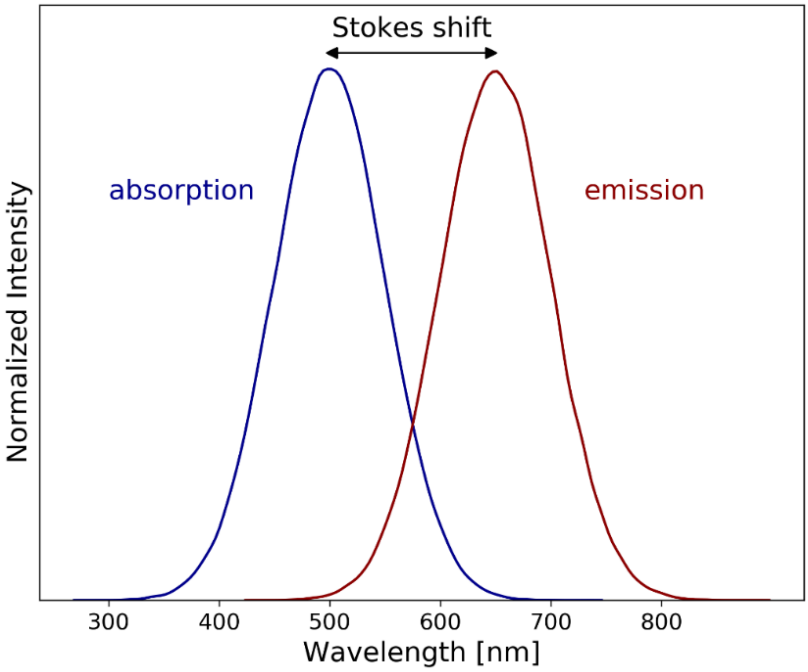

Figure 2. Excitation and emission spectra with a Stokes shift of ~150 nm.

However, in rare cases when excitation happens not from the ground state but from the higher vibrational levels, emitted photons can eventually have larger energy than absorbed ones [25]. This phenomenon is logically called anti-Stokes shift, and it is typically investigated within the scope of Raman spectroscopy [25].

To conclude, when investigating luminescence properties of the sample, first, the emission spectrum is recorded to determine the emission color and maximum of the sample [29]. Then, the excitation spectrum is recorded to select a suitable excitation wavelength for luminescence emission lifetime and quantum yield measurements [26].

1.2.2 Luminescence emission lifetime

Luminescence emission lifetime is mean time a molecule spends at an excited state [26]. For fluorophores, typical emission lifetime values are around 10^{-8} seconds [26]. For phosphors, emission lifetime values are typically near 10^{-2} seconds, but much longer values are also not uncommon [25,26].

In most cases, emission lifetime follows first-order kinetics [25]. It means that it can be calculated by fitting single-exponential decay function to measured emission decay curve:

$$I(t) = A_0 \cdot \exp(-t/\tau_0), \tag{1}$$

where $I(t)$ is the luminescence intensity at a given time t, A_0 is a pre-exponential factor, and τ_0 is the emission lifetime [30].

In cases where emission have multiple components (*e.g.*, a mixture of compounds or competing mechanisms of emission), a multi-exponential model must be used:

$$I(t) = \sum_{\mathrm{i}=1} A_{\mathrm{i}} \cdot \exp(-t/\tau_{\mathrm{i}}) \tag{2}$$

In the case of bi-exponential decay function, the average emission lifetime is, therefore:

$$\tau_{\mathrm{av}} = \frac{A_1\tau_1^2 + A_2\tau_2^2}{A_1\tau_1 + A_2\tau_2}, \tag{3}$$

where τ_{av} is the average emission lifetime.

1.2.3 Luminescence quantum yield

Luminescence quantum yield (Φ), sometimes called quantum efficiency, describes the ratio between radiative and non-radiative relaxation processes in luminescent materials [25]. It is a crucial parameter for the performance evaluation of luminescent materials [27]. Φ can be expressed with the following formula:

$$\Phi = \frac{\text{Number of photons emitted}}{\text{Number of photons absorbed}} \tag{4}$$

The larger value of Φ, the more photons a material emits, hence the more intense is the luminescence of material. For luminescent phosphors used in commercial light-emitting devices, Φ values of 0.50–0.90 are typical [25].

Φ can be measured directly, by detecting the emitted photons (optical methods), or indirectly, by measuring the increase in temperature arising from vibrational relaxation (photothermal or

calorimetric methods) [27]. When using optical methods, Φ of a sample can be measured in comparison to a standard with a known Φ. In this way, a relative Φ value is obtained. Measurements of relative Φ can be inaccurate due to the complexity of instrument calibration and sensitivity of measured Φ to the Φ value of a standard sample.

To obtain the absolute Φ value, setups equipped with an integrating sphere can be used [27]. Integrating sphere is apparatus, which collects all photons transmitted, scattered, and emitted by the sample; collected photons are then directed to the detection system [27]. As an excitation light source, a xenon lamp with a monochromator, laser, or LED are commonly used [27]. Samples are measured in comparison to the blank, which is used to exclude the influence of the environment. As with relative Φ measurements, negligent calibration of integrated sphere setup can considerably influence the results. Thus, measurements of blank and sample must be done under the same conditions, *i.e.*, at constant temperature and with the same ambient light. It is also important to use sample holders made of the same material for both blank and sample measurements [27]. In most cases, non-luminescent quartz sample holders are used for the integrated sphere measurements [11,27]. Another source of uncertainty for integrated sphere setup is the possible reabsorption of emitted light, which leads to underestimation of Φ [27]. This effect can be reduced by more careful optimization of measurement setup [31]. It is also possible to exclude the impact of reabsorption from the results by using special mathematical techniques [32].

In the current study, a measurement setup equipped with an integrated sphere was used to measure the absolute quantum yield of prepared complexes.

1.3 Anionic Pt(II) complexes

Since the discovery of cisplatin's (*cis*-$Pt(NH_3)_2Cl_2$) anticancer activity in the late 1960s, the development of new Pt(II) complexes was actively driven by their use in biological systems [33,34]. Due to the active interest and financing from the medicine sector, the main ligand types and synthesis routes used till now for Pt(II) complexes were discovered during the 1980s and 1990s [35–39]. It was demonstrated then that pyridine-based bidentate chelating ligands (see Figure 3), such as 2-phenylpyridine (PPy), 2,2'-bipyridine (BPy) and 2-(2-thienyl)pyridine (ThPy) form exceptionally stable cyclometalated Pt(II) complexes [36,37,39,40].

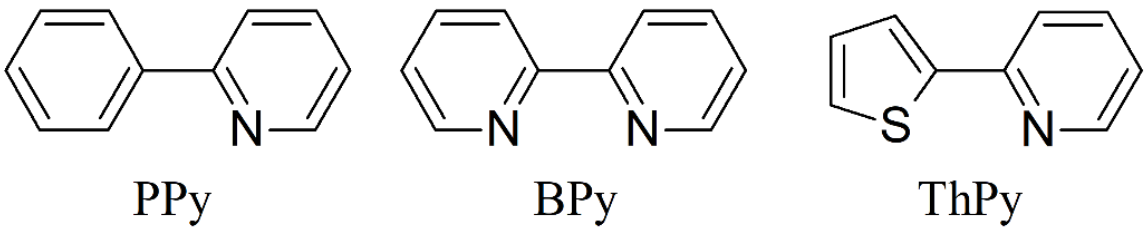

Figure 3. Common pyridine-based ligands of cyclometalated Pt(II) complexes.

Luminescence of some synthesized cyclometalated Pt(II) complexes was also reported [35–37]. Yet it was not until the 2000s when the more thorough investigation of the luminescence of Pt(II) complexes started, driven mainly by the field of novel light-emitting systems, such as OLEDs and LEECs [34,41,42]. Currently, research in this field is concentrating on studying the luminescence mechanisms of known Pt(II) complexes [43–45], as well as on preparing new complexes with higher luminescence intensity [41,46]. Especially anionic Pt(II) complexes (see Figure 4) have attracted much attention due to their increased solubility compared to neutral Pt(II) complexes, which widens their possible applications, especially in optoelectronics and biomedicine [41].

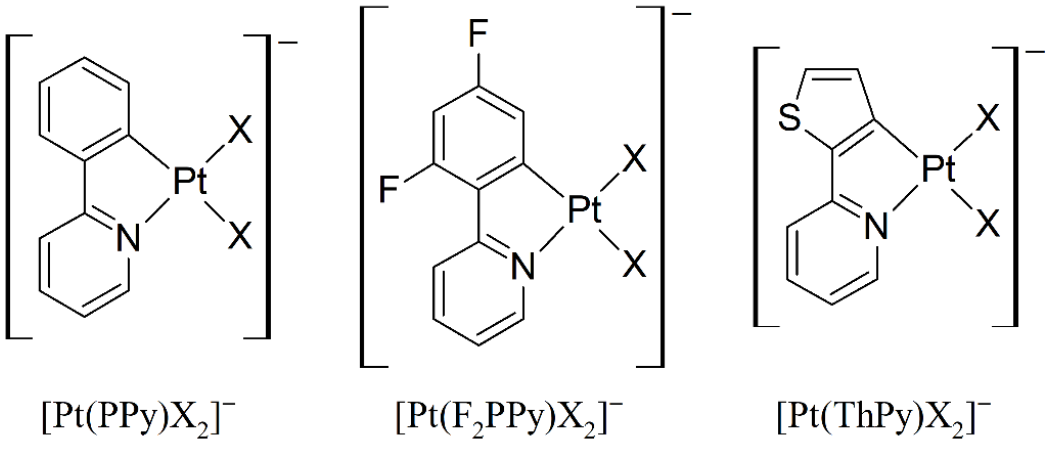

Figure 4. Typical anionic Pt(II) complexes [41]. X stands for negatively charged ligands (*e.g.*, Cl^- or CN^-).

Motivated by these emerging trends in the field, the current study focuses on preparation of new luminescent anionic Pt(II) complexes with PPy ligand. As intermediates, three neutral dimeric Pt(II) complexes are also synthesized.

1.4 Ionic liquids

ILs are usually defined as ionic compounds with a melting point under 100 °C, which differs from common molten salts [47]. The low melting point of ILs is ensured by the usage of bulky and asymmetric cations, which disturb formation of energetically stable crystal lattice. Typical cations used for preparation of ILs are 1-alkyl-3-methylimidazolium, 1-alkylpyridinium, tetraalkylammonium and tetraalkylphosphonium ions (see Figure 5) [47,48].

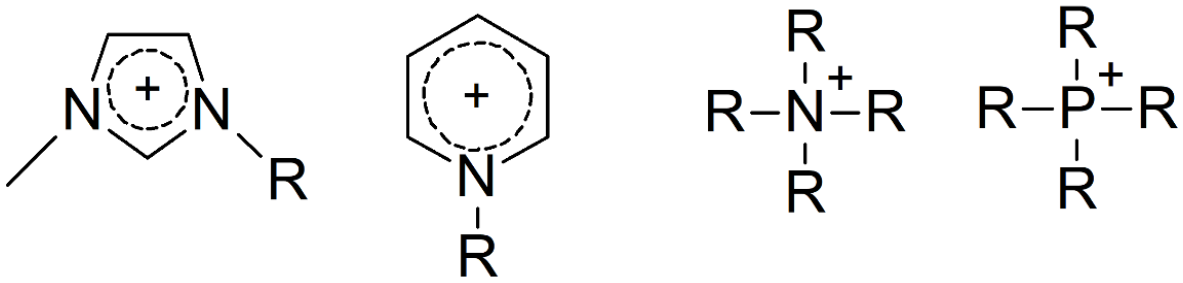

Figure 5. Structures of common cations of ionic liquids [47]. R stands for an alkyl group.

Although the first IL, ethylammonium nitrate, was discovered back in 1914, almost a century had passed till ILs became a topic of intense scientific research [47]. The first real application of ILs, introduced by Seddon and Hussey in the 1980s, was their use as nonaqueous and polar solvents, suitable for electrochemical experiments with transition metal complexes [47]. The work of Seddon and Hussey had set a research direction for ILs for decades. Nowadays, ILs are known as “alternative” solvents, referring to their use instead of more conventional organic solvents [47]. ILs had also obtained an environmentally friendly reputation, mainly due to their nonvolatile and nonflammable nature [49]. ILs are also easy to reuse, which increases their applicability as electrolytes and solvents [50].

Given the fact that the amount of possible cation and anion combinations suitable for the preparation of ILs is close to one trillion, it is crucial to decide desired properties of ILs prior to their synthesis and use [48]. One of the hottest areas in ILs research nowadays is synthesis of task-specific ILs with additional functionality [49]. To functionalize ILs, *d*- and *f*-metal complexes are often used as anions. Usage of anionic metal complexes allows to synthesize ILs with unique electrochemical, magnetic, or luminescent properties [10].

1.4.1 Luminescent ionic liquids

Lately, particularly LILs had attracted the attention of the scientific world due to their possible application in light-emitting systems or in temperature sensors [10–13,17,51–54]. Till now, to prepare LILs multiple *d*- and *f*-metal complexes were used [13,15,16,53,55,56]. However, LILs

reported so far have a common shortcoming of a low quantum yield, far from quantum yield values of commercially applied phosphors [10,25]. That is a crucial aspect to pay attention to because poor luminescent intensity limits possible applications of ILs in light-emitting systems. To address this problem, Ogawa *et al*. have turned their attention to anionic Pt(II) complexes, which are known for their luminescence intensity [10,11,35,41,57]. They synthesized three different LILs using three different Pt(II) complexes and characterized their luminescence properties at room temperature (RT) and 77 K [11]. Although LILs prepared by Ogawa *et al*. showed quantum yield values as high as 0.94 at 77 K, values at RT were around 0.10, which had yet left much to be desired [11]. Current study continues the work of Ogawa *et al*. in preparation of LILs based on anionic Pt(II) complexes, with an aim to improve emission quantum yield of final compounds.

1.5 Thermoanalytic techniques

With the melting temperature being a descriptor of high importance for ILs, it is crucial to measure it with special care. Among all the techniques being used for the determination of melting temperature, differential scanning calorimetry (DSC) and thermogravimetric analysis combined with differential thermal analysis (TG-DTA) are the most prominent and easy-to-use, especially for measurements of ILs [58–61].

Thermoanalytic techniques, such as DSC and DTA, are measuring changes in heat required to increase the temperature of a sample as a function of temperature or time [62]. Measurements are usually done in comparison to inert reference. In case of TG-DTA, differential analysis is combined with TG, which measures changes in sample weight simultaneously to the heat change measurement [63]. Both techniques have certain similarities, such as the necessity to thoroughly determine sample weight or to conduct the measurements under inert gas flow [62,63]. However, their application in ILs research has some noteworthy differences to mention. DSC is mainly used to determine melting and glass-transition points, as well as heat capacities and enthalpies of the ILs [58–61,64]. On the other hand, the main application of TG-DTA in the case of ILs is the evaluation of their thermal stability. Still, it also is capable of estimating melting points [63,65].

In the current study, DSC was used to measure melting and glass-transition points of synthesized ILs, while TG-DTA was used to measure melting points of the complexes with estimated melting points higher than 100 °C.

2 EXPERIMENTAL

2.1 Physical measurements

^{1}H nuclear magnetic resonance (NMR) spectra were measured using a JEOL EX-270 NMR spectrometer at a frequency of 400 MHz. All spectra are presented on points per million (ppm) scale. As solvents, deuterated chloroform (chloroform-d) or dimethyl sulfoxide (DMSO-d_6) were used; tetramethylsilane (TMS) was used as a primary reference (0 ppm). Solvents and the reference were purchased from Kanto Chemical Co., Inc.

Samples of final products were also sent for an additional purity control via elemental analysis to the Analysis Center in Hokkaido University.

TG-DTA was performed using a Rigaku Thermoplus EVO TG-DTA 8120. Measurements were done in the range from room temperature to 200 °C under Ar flow (0.3 L/min); scan rate was 1–2 °C/min. Aluminum pans were used as a sample holder, and Al_2O_3 powder was used as an inert reference.

DSC was carried out using a METTLER DSC 1 calorimeter under N_2 flow (0.06 L/min). Measurements were done using closed Al sample pans; as a coolant, liquid N_2 was used. Samples were analyzed in temperature range from –70 °C to 70–110 °C, depending on the expected melting point; the scan rate for all samples was 5 °C/min.

2.2 Synthesis procedure

Information on reagents, materials, and solvents used is concluded in Appendix 1. Structures of all six target complexes can be found in Appendix 2.

2.2.1 [Pt(η^3-methylallyl)Cl]$_2$

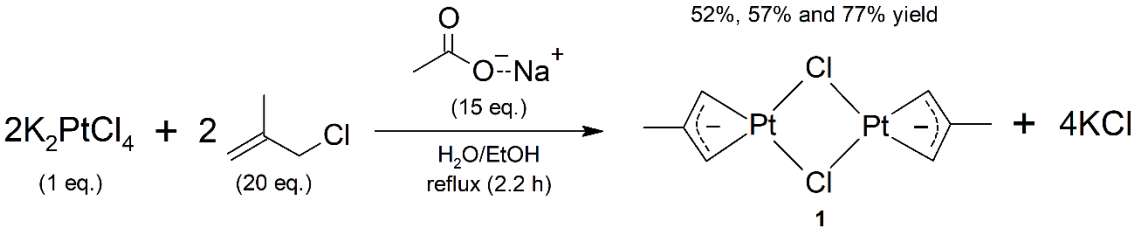

Figure 6. Synthesis of [Pt(η^3-methylallyl)Cl]$_2$ (**1**).

To synthesize first intermediate complex, [Pt(η^3-methylallyl)Cl]$_2$ (**1**), route adopted from Mabbott *et al*. was used (see Figure 6) [38]. By this route, sodium acetate (2.8251 g, 35 mmol) and 3-chloro-2-methylpropene (4 mL, 41 mmol) were added to 60 mL of ethanol and heated

until the mixture started to boil. In another flask, potassium tetrachloroplatinate (K_2PtCl_4, 0.808 g, 1.94 mmol) was added to 8 mL of H_2O, stirred in an ultrasonic bath (180 W, 44 kHz) for 1 minute, heated to 70 °C, to ensure complete dissolution, and added to ethanol solution. The resulting mixture was heated on reflux for 2.2 hours, then cooled down to RT, and solvent was removed on the rotary evaporator (50 °C, 40 torr). Obtained solid was extracted with dichloromethane (DCM) (once with 20 mL, three times with 10 mL), all fractions collected and dried on Na_2SO_4. Next, Na_2SO_4 was removed by filtration, and DCM was removed on the rotary evaporator (40 °C, 400 torr). The resulting brown sticky residue was treated with diethyl ether (three times with 10 mL) and dried overnight *in vacuo*. As a result, 0.2894 g (52% yield) of brown solid, $[Pt(\eta^3\text{-methylallyl})Cl]_2$ (**1**), was obtained.

The structure of the product was confirmed by comparing measured ^1H NMR spectrum (see Appendix 3) to the published one [66]; (chloroform-d, 400 MHz) δ 3.69 (t, J = 19.4 Hz, 3H), 2.18 (q, J = 20.4 Hz, 4H) ppm.

This reaction was repeated twice afterward, with the same conditions and quantities, resulting in similar yields: 0.3300 g (58% yield) and 0.5257 g (77% yield) of complex **1** were obtained as a result.

2.2.2 $[Pt(PPy)Cl]_2$

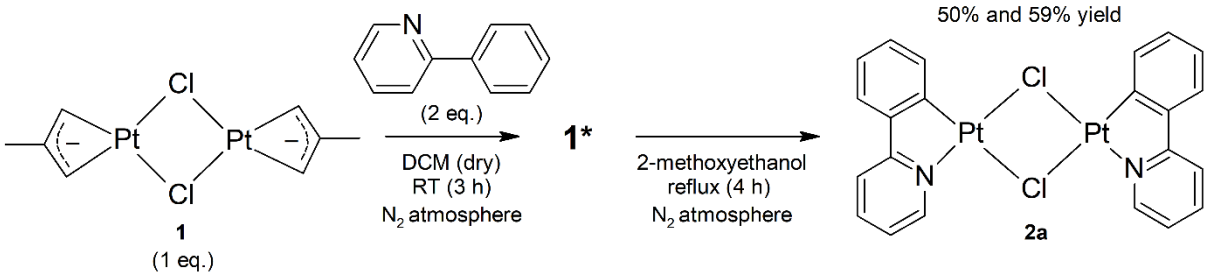

Figure 7. Synthesis of $[Pt(PPy)Cl]_2$ (**2a**).

To conduct ligand exchange reaction of complex **1** with 2-phenylpyridine (PPy), a route adopted from Romero *et al*. was initially tried [67]. In accordance with their experimental procedure, PPy was added to a suspension of complex **1** in dry toluene and heated under reflux for 2 h [67]. However, this route was found to be unsuitable, with most of the complex **1** decomposing and precipitating as colloidal Pt. Eventually, a milder synthesis route was developed by following the synthetic method for similar compounds adopted from Fuertes *et al*. (see Figure 7) [68]. For the reaction, 0.3300 g of complex **1** (see Figure 7) and 165 µL of PPy were dissolved in 50 mL of dry DCM (bubbled with N_2 and held on 4 Å molecular sieves for

48 hours) and mixed at RT under N_2 flow for 3 hours. After that, the solvent was removed, and the residue was washed with hexane (twice with 20 mL). Obtained intermediate complex (**1***) was then dissolved in 12 mL of 2-methoxyethanol and heated under reflux for 4 hours under N_2 flow to promote complete attachment of PPy ligand to Pt atom. Fine powder, formed during this reaction, was separated by centrifugation. The obtained residue was then washed with DCM (twice with 5 mL) and diethyl ether (once with 5 mL) and dried overnight *in vacuo*. As a result, 0.2223 g (50% yield) of fine greenish powder, $[Pt(PPy)Cl]_2$ (**2a**), was obtained.

Formation of cyclometalated complex and the purity of product were confirmed by ^1H NMR spectrum (see Appendix 3); (DMSO-d_6, 400 MHz) δ 9.49 (d, *J* = 5.8 Hz, 1H), 8.23 (d, *J* = 7.6 Hz, 1H), 8.18-8.12 (m, 2H), 7.79 (d, *J* = 7.4 Hz, 1H), 7.53 (t, *J* = 6.3 Hz, 1H), 7.20-7.11 (m, 2H) ppm.

This reaction was repeated later under the same conditions with 0.4621 g of complex **1**, resulting in 0.3675 g of $[Pt(PPy)Cl]_2$ (**2a**) (59% yield) of the same purity.

2.2.3 Complexes with $[Pt(PPy)Cl_2]^-$ anion (3a–3c)

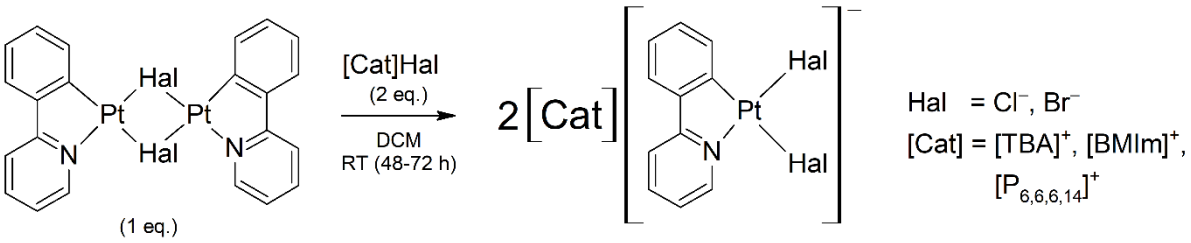

Figure 8. General synthesis scheme for complexes **3a**–**3b**, **4a**–**4c**.

To synthesize complexes **3a**–**3b**, a route adopted from Kvam and Songstad was used (see Figure 8) [39].

In the case of complex **3a** (see exact scheme at Appendix 4), 73.6 mg of dimer **2a** and 99.6 mg of trihexyltetradecylphosphonium chloride, $[P_{6,6,6,14}]Cl$, were added to 5 mL of DCM and mixed at RT for 72 hours, resulting in a pale yellow solution. The obtained solution was filtered through a membrane filter, and DCM was removed on the rotary evaporator (40 °C, 400 torr). As a result, yellow viscous liquid was obtained. It was left to dry under vacuum for three days, slowly crystallizing and resulting in 172.8 mg (100% yield) of greenish yellow solid, $[P_{6,6,6,14}][Pt(PPy)Cl_2]$ (**3a**).

Formation of new complex and purity of the product were confirmed by ^{1}H NMR spectrum (see Appendix 3); (chloroform-d, 400 MHz) δ 9.94 (d, *J* = 5.8 Hz, 1H), 8.09 (d, *J* = 7.7 Hz, 1H), 7.75 (td, *J* = 7.7, 1.3 Hz, 1H), 7.54 (d, *J* = 7.9 Hz, 1H), 7.34 (dd, *J* = 7.5, 1.2 Hz, 1H), 7.07-7.00 (m, 3H), 2.43 (m, 8H), 1.38-1.21 (m, 48H), 0.87 (m, 12H) ppm.

Elemental analysis showed following atomic composition: C, 56.74%; H, 8.43%; N, 1.46%, which is almost identical to the calculated atomic composition of partially hydrated complex form, $[P_{6,6,6,14}][Pt(PPy)Cl_2]\cdot 0.5H_2O$: C, 56.57%; H, 8.50%; N, 1.53%. Hence, complex **3a** is a hygroscopic compound with a water content of about 1%, which is common for ILs [69,70].

Complex **3b** was synthesized analogously with complex **3a**, by mixing 1-butyl-3-methylimidazolium chloride, [BMIm]Cl, and dimer **2a** in DCM (see Figure 8). For details on quantities and ratios of starting materials for this and other syntheses, please refer to Appendix 5. After three days of drying *in vacuo*, 118.8 mg (102% yield) of **3b** was obtained as greenish yellow liquid. Elemental analysis of this sample showed presence of impurities (presumably water and some leftovers of [BMIm]Cl), which were removed by extraction with diethyl ether, resulting in 116.4 mg (98% yield) of dark greenish yellow solid, $[BMIm][Pt(PPy)Cl_2]$ (**3b**). The purity and structure of the product were then confirmed by elemental analysis and ^{1}H NMR spectrum (see Appendix 6).

Synthesis of **3b** was later repeated, resulting in 77.5 mg (99% yield) of neat product.

Complex **3c**, which was already reported before, was synthesized following an alternative route, derived from Craig *et al*. (for details see Appendix 7) [35]. The synthesis was repeated twice under the same conditions. In total, 88.6 mg (12% yield) + 197.6 mg (12% yield) of neon yellow crystals, $[TBA][Pt(PPy)Cl_2]$ (**3c**), were obtained.

2.2.4 Complexes with $[Pt(PPy)Br_2]^-$ anion (4a–4c)

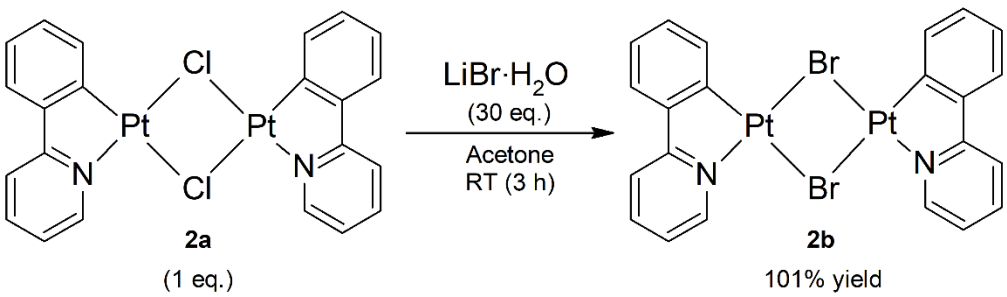

Figure 9. Synthesis of $[Pt(PPy)Br]_2$ (**2b**).

To synthesize complexes **4a**–**4c**, chlorine in halogen-bridge of complex **2a** had to be replaced with bromine. This was done by introducing halogen-bridge cleavage reaction, analogous to the synthesis method developed by Black *et al*. (see Figure 9) [71]. For this reaction, 821.2 mg of lithium bromine monohydrate was dissolved in 60 mL of acetone, and then 200.0 mg of complex **2a** was added to the solution. The resulting mixture was stirred at RT for 3 hours, then concentrated on the rotary evaporator. The obtained yellow residue was treated with 20 mL of methanol and water mixture (1:1), filtered, washed first with methanol, then with diethyl ether, and dried overnight *in vacuo*. Finally, 225.4 mg (101% yield) of a pale yellow powder, $[Pt(PPy)Br]_2$ (**2b**), was obtained. Purity of product and formation of new halogen bridge were confirmed by ^{1}H NMR (see Appendix 3); (DMSO-d_6, 400 MHz) δ 9.77 (d, *J* = 5.6 Hz, 1H), 8.27 (d, *J* = 8.0 Hz, 1H), 8.18-8.12 (m, 2H), 7.79 (d, *J* = 7.6 Hz, 1H), 7.50 (t, *J* = 6.2 Hz, 1H), 7.22-7.15 (m, 2H) ppm. Slightly heightened yield can hence be explained with some leftovers of solvents or washing water.

Complexes **4a**–**4c** were synthesized following analogous synthesis route as with complexes **3a** and **3b** (see general scheme at Figure 8). Precise information about the quantities of starting materials for those syntheses is concluded in Appendix 5. The results were as follows:

$[P_{6,6,6,14}][Pt(PPy)Br_2]$ (**4a**), dark yellow solid, 175.4 mg (97% yield).

$[BMIm][Pt(PPy)Br_2]$ (**4b**), dark yellow solid, 90.8 mg (98% yield).

$[TBA][Pt(PPy)Br_2]$ (**4c**), dark yellow powder, 104.4 mg (98% yield).

Synthesis of complexes **4b** and **4c** was repeated once under similar conditions, resulting in 76.4 mg (93% yield) and 166.2 mg (99% yield) of neat products accordingly.

The structure and purity of **4a**–**4c** were also confirmed by ^{1}H NMR spectra and elemental analysis. These results are concluded in Appendix 6.

2.3 Luminescence measurements

Luminescence properties of synthesized complexes **3a**–**3c** and **4a**–**4c** were investigated by measuring their emission spectra, emission lifetime, and quantum yield at RT and at 77 K. For complexes **3a** and **4a**, luminescence properties of two additional states, supercooled liquid (at RT) and glass (at 77 K), were investigated as well.

2.3.1 Luminescence spectra

Luminescence spectra were measured with JASCO FP-8600 spectrofluorometer with a xenon lamp excitation light source and a slit width of 10 nm. For emission spectra of all complexes, excitation wavelength of 350 nm and cut-off filter of 370 nm were found to be optimal. For excitation spectra, emission wavelengths were derived from emission maxima, and cut-off filters of 490 nm or 520 nm were chosen, depending on emission maxima values. At 77 K measurements were conducted under N_2 atmosphere.

2.3.2 Luminescence quantum yield

Luminescence absolute quantum yields (Φ) were measured with Hamamatsu Photonics C9920-02 equipped with integrated sphere apparatus; xenon lamp and a monochromator were used as an excitation light source. The accuracy of a setup was controlled by measuring the Φ of a reference solution with a known Φ value (anthracene in ethanol, Φ = 0.27) [72]. All Φ measurements were done at the excitation maxima of samples derived from excitation spectra. For each sample, the Φ was calculated from an average of five measurements.

2.3.3 Luminescence emission lifetime

Emission lifetime measurements were done using two different systems: Hamamatsu Quantaurus-Tau C11367 for RT measurements and Hamamatsu Photonics C4334 for measurements at 77 K. Hamamatsu Quantaurus-Tau C11367 was equipped with an LED lamp and monochromator, and measurements were conducted at the excitation wavelength of 365 nm. Hamamatsu Photonics C4334 system had a laser with the light wavelength of 337 nm as an excitation light source and a streak camera as a photodetector.

For all emission decay curves the single-exponential model was applied. If the model fit, pre-exponential factors (A_0) and emission lifetimes (τ_0) were calculated from Equation 1. Otherwise, bi-exponential model was applied, and pre-exponential factors (A_1 and A_2) as well as the average emission lifetimes (τ_{av}) were calculated from Equation 3.

2.4 Photographic and video materials

For preparing photographic and video materials on synthesized complexes, Keyence VHX-600 digital microscope equipped with Linkam THMS600 temperature control stage was used. Photographs and video were taken under ambient and ultraviolet (UV) light. As an UV light source, UV-LED flashlight with 375 nm light was used.

3 RESULTS AND ANALYSIS

In previous research on LILs based on anionic Pt(II) complexes, Ogawa *et al*. succeeded to prepare three new ILs, however, their absolute quantum yield at RT left much to be desired [11]. In current study, nine Pt(II) complexes were successfully prepared, of which six (**2b**, **3a**, **3b** and **4a**–**4c**) are previously unreported compounds. To determine melting point of complexes **3a**–**3c** and **4a**–**4c**, DSC or TG-DTA measurements were conducted. To investigate luminescence properties, emission, and excitation spectra, as well as the emission lifetime and quantum yields, were measured. To get deeper insight on the origins of emission, luminescence properties were measured at RT and 77 K for crystal states. In case of complexes **3a** and **4a** luminescence properties were also measured for glass and liquid states where available.

3.1 Thermal properties

Melting points (T_m) obtained from DSC or TG-DTA measurements, as well as glass-transition temperatures (T_g) obtained from DSC measurements, are concluded in Table 1.

Table 1. Thermal properties of neat **3a**–**3c** and **4a**–**4c**.

Complex	T_m (°C)	T_g (°C)
$[P_{6,6,6,14}][Pt(PPy)Cl_2]$ (**3a**)	50	−48
$[P_{6,6,6,14}][Pt(PPy)Br_2]$ (**4a**)	50	−55
[BMIm][Pt(PPy)Cl_2] (**3b**)	85	−25
[BMIm][Pt(PPy)Br_2] (**4b**)	69	−24
[TBA][Pt(PPy)Cl_2] (**3c**)	185	-
[TBA][Pt(PPy)Br_2] (**4c**)	170	-

Melting points (T_m) of complexes **3a** and **4a** were estimated by DSC from the endothermic peaks of 2nd heating cycle (see Figure 10 (a) and Appendix 8).

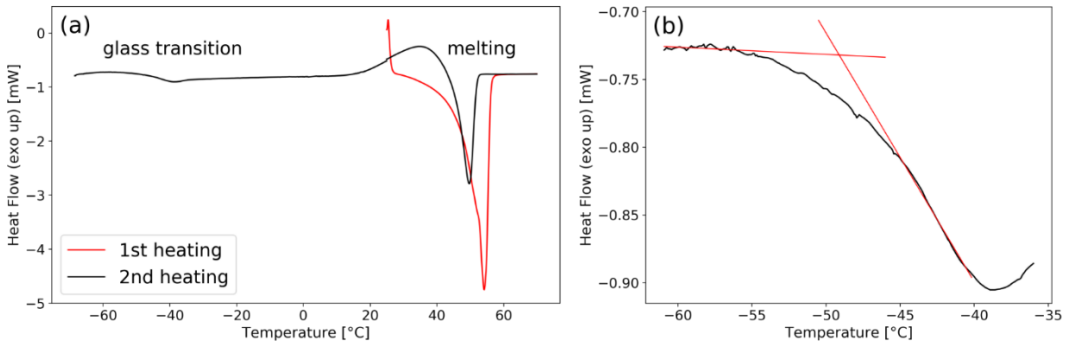

Figure 10. (a) DSC curve of complex **3a** and (b) corresponding magnified DSC curve.

In the case of complexes **3b** and **4b**, no crystallization occurred on cooling, which is not uncommon for imidazolium-based ILs [59]. Therefore, T_m of **3b** and **4b** were estimated from the endothermic peaks of the 1st heating cycle (see Appendix 8).

Glass-transition temperatures (T_g) were estimated from the steps in the baselines of the DSC curves; an example of the fitting process can be seen in Figure 10 (b).

For complexes **3c** and **4c** melting points were roughly estimated to be larger than 100 °C by failed melting attempt with hot air gun set to 110 °C. Then, TG-DTA measurement was conducted, and precise melting point values were obtained from the endothermic peaks of DTA curves (see Figure 11).

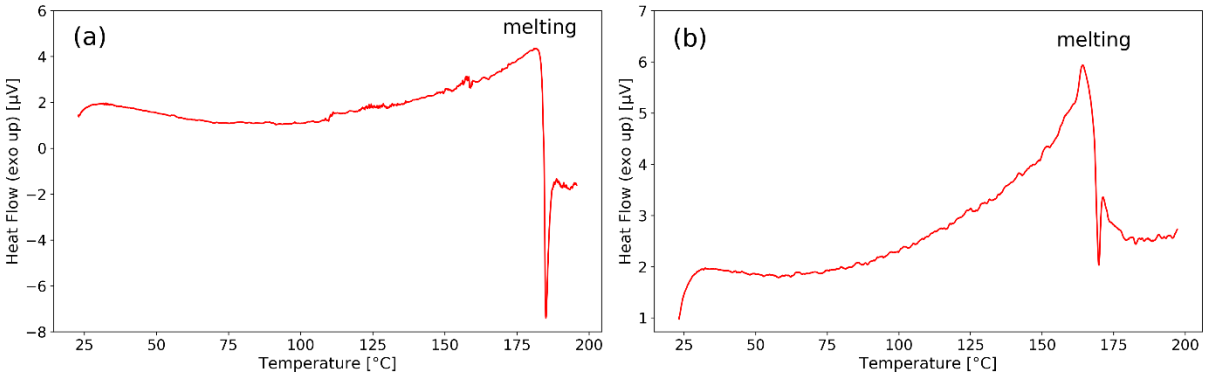

Figure 11. DTA curves for (a) complex **3c** and (b) complex **4c**.

As indicated in the Table 1, complexes **3a**–**4a** and **3b**–**4b** (with $[P_{6,6,6,14}]^+$ and $[BMIm]^+$ cations respectively) have a melting point below 100 °C and therefore are qualified as ILs. It is also noteworthy that those complexes have glass-transition temperatures above 77 K, which made it possible to measure their luminescence properties at glass state by using liquid nitrogen as a coolant.

3.2 Luminescence properties

Results of luminescence measurements done are concluded in a Table 2.

Table 2. Photophysical data of neat **3a**–**3c** and **4a**–**4c** at 298 K and 77 K.

Complex, state	T (K)	λ_{em}^{max} (nm)	Φ[a]	τ[b] (μs)
$[P_{6,6,6,14}][Pt(PPy)Cl_2]$ (**3a**), liquid	298	541	0.01	NA[c]
$[P_{6,6,6,14}][Pt(PPy)Cl_2]$ (**3a**), glass	77	505	0.52	6.3
$[P_{6,6,6,14}][Pt(PPy)Cl_2]$ (**3a**), crystal	298	539	0.40	3.1
	77	504	0.71	6.4
$[P_{6,6,6,14}][Pt(PPy)Br_2]$ (**4a**), liquid	298	537	0.01	NA
$[P_{6,6,6,14}][Pt(PPy)Br_2]$ (**4a**), glass	77	542	0.33	4.9
$[P_{6,6,6,14}][Pt(PPy)Br_2]$ (**4a**), crystal	298	537	0.04	0.4
	77	540	0.55	6.4
[BMIm][Pt(PPy)Cl$_2$] (**3b**), crystal	298	542	0.04	0.5
	77	503	0.65	5.1
[BMIm][Pt(PPy)Br$_2$] (**4b**), crystal	298	540	0.02	0.1
	77	501	0.45	4.8
[TBA][Pt(PPy)Cl$_2$] (**3c**), crystal	298	540	0.49	3.2
	77	536	0.63	5.5
[TBA][Pt(PPy)Br$_2$] (**4c**), crystal	298	541	0.02	0.2
	77	507	0.55	4.4

[a]Φ: emission quantum yield. [b]τ: emission lifetime.
[c]NA: not available, because of too low value

3.2.1 Luminescence spectra

As listed in Table 2, emission maxima (λ_{em}^{max}) of all complexes are at around 505 nm or 540 nm, depending on the state of a complex and measurement temperature. Measurements of emission spectra showed that all complexes exhibit the strongest emission at a wavelength interval of 500–600 nm, which corresponds to green light emission. It was also found that the shape of the emission spectra of all six complexes at RT is practically the same (see Figure 12). This is logical because the emission should originate from the interaction of Pt(II) with PPy ligand and this ligand is the same for all prepared complexes.

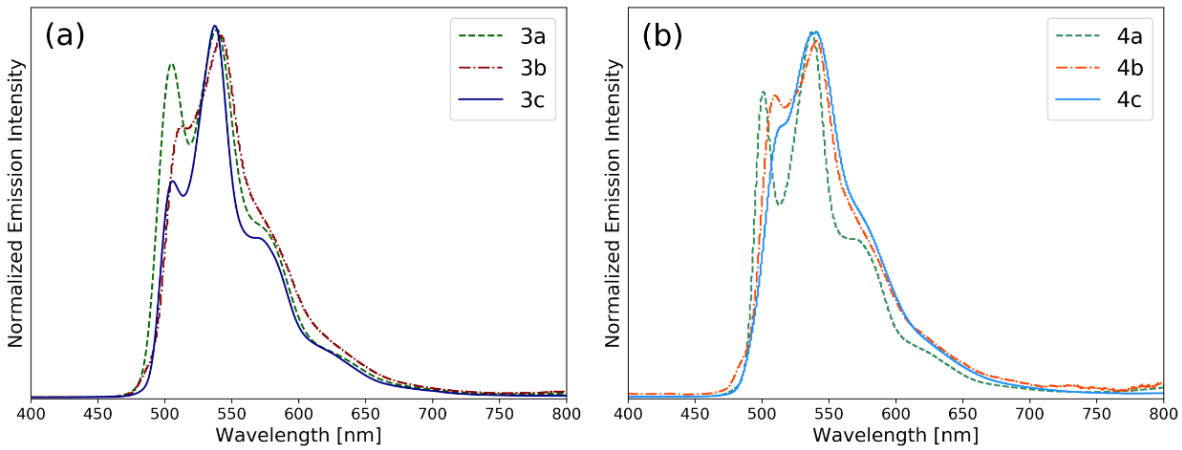

Figure 12. Emission spectra of complexes (a) **3a**–**3c** and (b) **4a**–**4c** at crystal state at RT.

Next, emission spectra at RT and 77 K were compared. It was observed that, in general, peak shape became sharper at 77 K. This effect is most noticeable in the case of complexes **3b** and **4b** (see Figure 13).

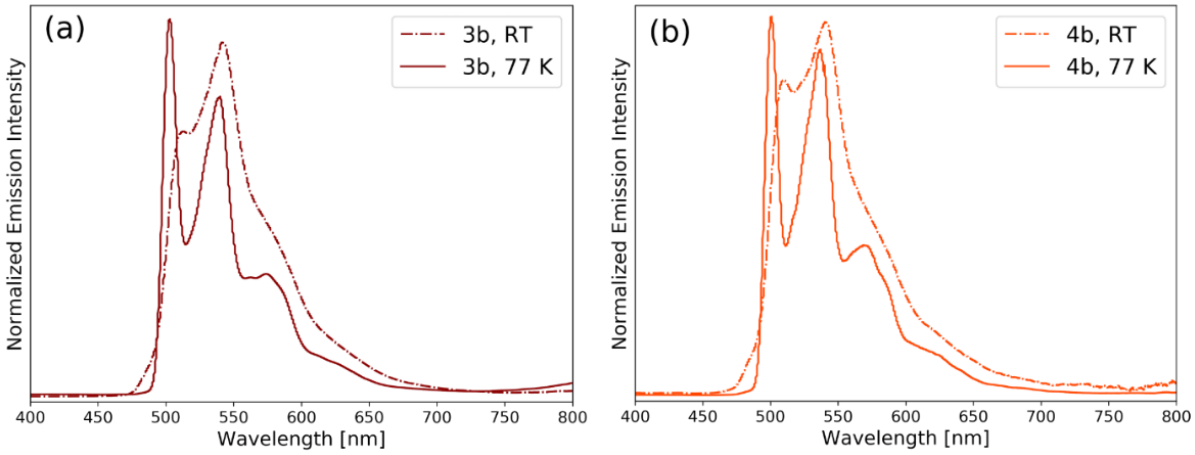

Figure 13. Emission spectra of complexes (a) **3b** and (b) **4b** at crystal state at RT and 77 K.

The sharpening of emission peaks while lowering the temperature can be attributed to increasing order of crystal lattice [35]. At lower temperatures, metal complexes become more rigid, which leaves fewer opportunities for vibrational relaxation. This leads to a reduction of the amount of available energy levels and sharpening emission peaks.

For complexes **3a** and **4a,** in addition to luminescence spectra of crystal state, spectra of glass and liquid states were measured. For both complexes, crystal states had shown more intense emission at 77 K compared to the glass states (see Figure 14). This result is logical because interatomic interactions in highly ordered crystalline solids should be stronger compared to the amorphous structure of glasses. Therefore, the luminescence of crystals should also be stronger.

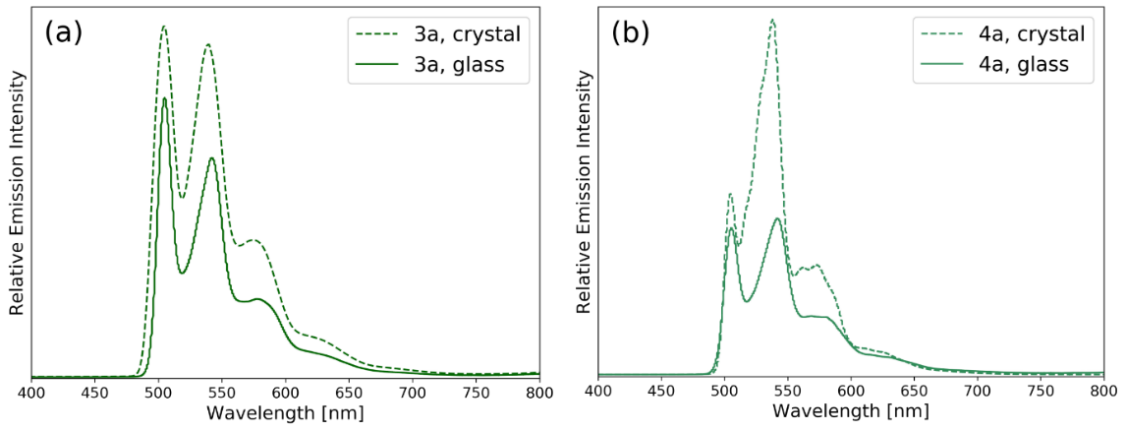

Figure 14. Emission spectra of complexes (a) **3a** and (b) **4a** at crystal and glass states at 77 K.

3.2.2 Luminescence emission lifetime

For the liquid state of complexes **3a** and **4a**, emission lifetime measurement could not be done because of technical limitations. Hamamatsu Quantaurus-Tau C11367 measurement system is more suitable for samples, which have a long emission lifetime. For poor luminescent samples with a shorter emission lifetime, the duration of measurement with this system tends to be too long and obtained data too noisy. Therefore, when the predicted length of emission lifetime measurement for **3a** and **4a** at liquid state with Hamamatsu Quantaurus-Tau C11367 system exceeded 90 minutes, it was decided to omit the experiment. However, this issue can be solved in future research by preparing larger sample bulks or by using a more sensible emission lifetime measurement system specifically developed for measurements of liquids.

Measurements of solid states of all complexes were successful, and the emission decay curves (see for example Figure 15) were analyzed using single-exponential or bi-exponential model (see Equations 1 and 2); average emission lifetimes (τ_{av}) were calculated using Equation 3.

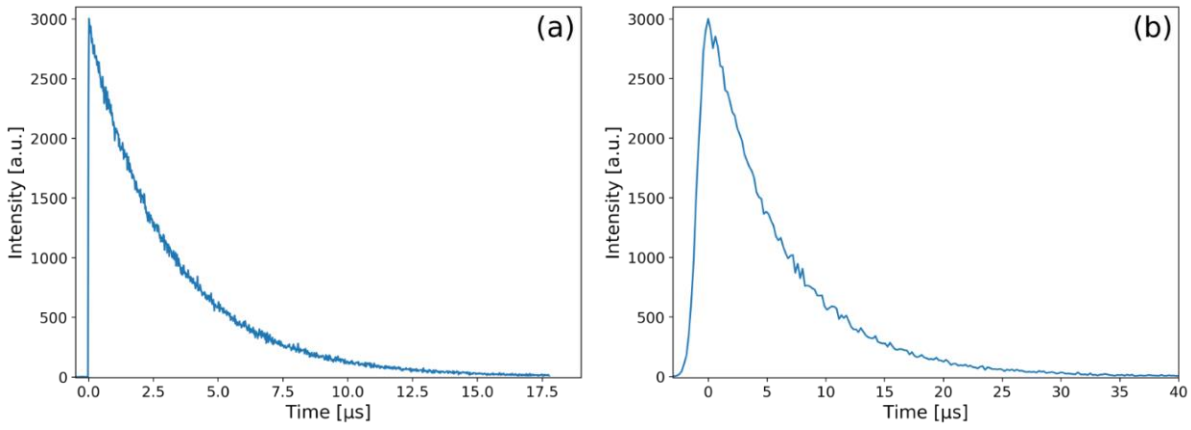

Figure 15. Emission decay curves of **3a** at (a) RT (λ_{ex} = 365 nm, A_0 = 2.7, τ_0 = 3.1 µs) and (b) 77 K (λ_{ex} = 337 nm, A_0 = 1.0, τ_0 = 6.4 µs).

Analysis of emission decay curves showed that emission lifetime of synthesized complexes is temperature dependent, with the emission lifetime being noticeably longer at 77 K, than at RT (see Table 2 and Figure 15). This effect can be explained with the shortening of atomic bonds at lower temperatures, which leads to a decrease of vibrational relaxation of molecules and therefore increasing emission lifetime [73,74].

To get numerical values for the difference in luminescence intensities of prepared complexes, emission absolute quantum yield was measured next.

3.2.3 Luminescence quantum yield

The emission absolute quantum yield (Φ) of synthesized complexes was also found to be strongly dependent on temperature, with the Φ values of all complexes at 77 K being remarkably higher, than at RT. This effect can be attributed to the shortening of atomic bonds at lower temperature, which suppresses non-radiative decay processes and therefore leads to an increase in luminescence intensity.

For complexes **3a** and **4a**, also the Φ dependence on state was investigated. As can be seen from Table 2, in case of complex **3a** the difference in Φ of crystal and liquid states at RT is significant, with Φ of the crystal state being about 40 times larger than that the one of the liquid state. However, for the complex **4a** this is not the case, which is most probably associated to the effect of bromine ligands. Φ measurement of glass and crystal states at 77 K for complexes **3a** and **4a** confirmed emission intensity difference, previously observed in emission spectra measurement (see Figure 14). As for the numerical difference, Φ values at 77 K of complexes **3a** and **4a** were about one-third larger at crystal state, than at glass state.

As indicated in Table 2, two out of prepared complexes had the Φ above 0.20 at RT. The one with largest Φ at RT is complex **3c**, previously reported compound [35], which was synthesized for current work as reference material. It is however the first time, when Φ yield for complex **3c** is reported. Second complex to have Φ above 0.20 is **3a**.

By closer investigation of Table 1 and Table 2 it is clear, that complex **3a** is surely most promising out of prepared complexes. It exhibits a remarkable Φ of 0.40 at RT, which is by an order of magnitude higher, than the measured Φ values at RT for other novel complexes synthesized in this work. The Φ value of 0.40 at RT is also almost four times larger, than the Φ values of similar LILs synthesized in previous works [11]. In addition, complex **3a** has a largest Φ value measured within this study: 0.71 at 77 K. Finally, melting temperature of

complex **3a** is 50 °C, which qualifies it as a LIL and hence fulfills the aim of current work. Low melting temperature facilitates production of thin films out of complex **3a** and prompts to its possible use as emitter in display and sensor devices. On the other hand, complex **3c** also has high Φ values, but its melting temperature of 185 °C limits its applicability for production of novel optoelectronic devices.

3.3 Influence of bromine ligand

In addition to rather obvious conclusions about Φ dependence on temperature and state, more intriguing observation can be done about the effect of bromine ligand on luminescence intensity of prepared complexes. As mentioned before, Φ of complex **4a** at RT was significantly smaller than the value for complex **3a**. Closer look to a Table 2 reveals, that introducing bromine ligand instead of chlorine had drastically reduced both Φ and emission lifetime at RT not only for complex **4a,** but also for **4c**. At 77 K the difference in luminescence intensities of complexes **3a**–**4a** and **3c**–**4c** is significantly smaller. This influence of bromine ligand can be explained with the weaker ligand field of bromine, which decreases the energy level of metal-centered excited state, opening a new pathway to non-radiative decay processes [73,75]. At lower temperatures this non-radiative decay pathway is suppressed due to the shortening of atomic bonds. Therefore, destructive effect of bromine ligand on luminescence processes at 77 K should be smaller. However, in accordance with this logic, difference between Φ and emission lifetime of complexes **3b** and **4b** at RT should also be noticeable, but this is not the case. Complex **3b** was found to have much lower Φ and shorter emission lifetime at RT, than expected from the general trends observed. To explain this abnormality, a hypothesis based on structural characteristics of $[BMIm]^+$ cation was developed.

It is possible, that poor emission of complex **3b** at RT is related to the influence of $[BMIm]^+$ cation on the crystal structure of the complex. $[BMIm]^+$ cation is certainly bulky and asymmetrical molecule with multiple stable conformations, which disturbs the formation of proper crystal lattice [58,59,76]. This leads to a low melting temperature of salts containing $[BMIm]^+$ cation and it was one of the reasons for $[BMIm]^+$ cation to be selected for synthesizing complexes in current work. However, disturbed crystal lattice could result in a certain amorphousness of complex **3b** solid state. This could lead to activation of non-radiative decay processes and therefore result in a lower Φ and shorter emission lifetime. To confirm this assumption, a detailed study of complex **3b** crystal lattice using methods like powder X-ray diffraction could be conducted in the future.

In conclusion, to proof suggested explanation of the influence of bromine ligand on luminescence properties of prepared complexes, more careful and detailed analysis of crystal lattice of complexes **3b** and **4b** should be done. In addition, synthesizing analogous complexes with iodine ligand could reveal a larger picture. According to spectrochemical series, iodine is ligand with the weakest field compared to other halogens [77]. If the assumption that weak field ligands reduce luminescence emission intensity of anionic Pt(II) complexes is correct, then complexes with $[Pt(PPy)I_2]^-$ anion should have the lowest emission quantum yield and lifetime values.

3.4 Further investigation of complex $[P_{6,6,6,14}][Pt(PPy)Cl_2]$

Based on results of luminescence and melting point measurements, $[P_{6,6,6,14}][Pt(PPy)Cl_2]$ (**3a**) was chosen for further investigation, due to its high luminescence quantum yield values (Φ = 0.40 and 0.71 at RT and 77 K accordingly) and low melting temperature (T_m = 50 °C).

First, to illustrate remarkable luminescence properties of complex **3a**, it was photographed in different states under ambient and UV light via microscope with temperature controller (see Appendix 9).

3.4.1 $[P_{6,6,6,14}][Pt(PPy)Cl_2]$ as a temperature sensor

Next, variable temperature luminescence spectra were measured to study the possible application of complex **3a** as a temperature sensor (see Figure 16).

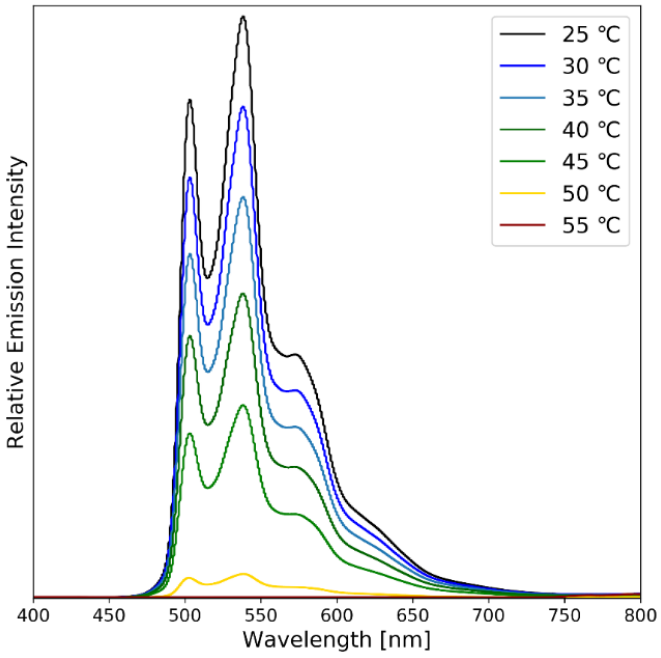

Figure 16. Variable temperature emission spectra of complex **3a**.

As can be seen from Figure 16, the luminescence intensity of complex **3a** is strongly dependent on temperature, with a critical point at around 50 ℃ at which complex **3a** melts and its luminescence intensity falls drastically. Those results prove that complex **3a** has a potential to be applied as a luminescent thermometer. Furthermore, drastic luminescence fall at around 50 ℃ can find application in temperature threshold detectors, which are meant to detect an overheat of a system and signal user about it [78]. A critical point of 50 ℃ is more than appropriate for most of the modern digital devices, such as smartphones or tablets, because at higher temperatures than that normal workflow of those devices can be interrupted and they can become harmful for users [79].

The next step was to investigate how fast does the complex **3a** crystallize and whether it restores its original luminescence intensity after numerous cycles of recrystallization. To do that, the Φ of **3a** at crystal state was measured, then crystals were melted, and rise of Φ in time was recorded with and without mechanical activation of the crystallization process (see Figure 17).

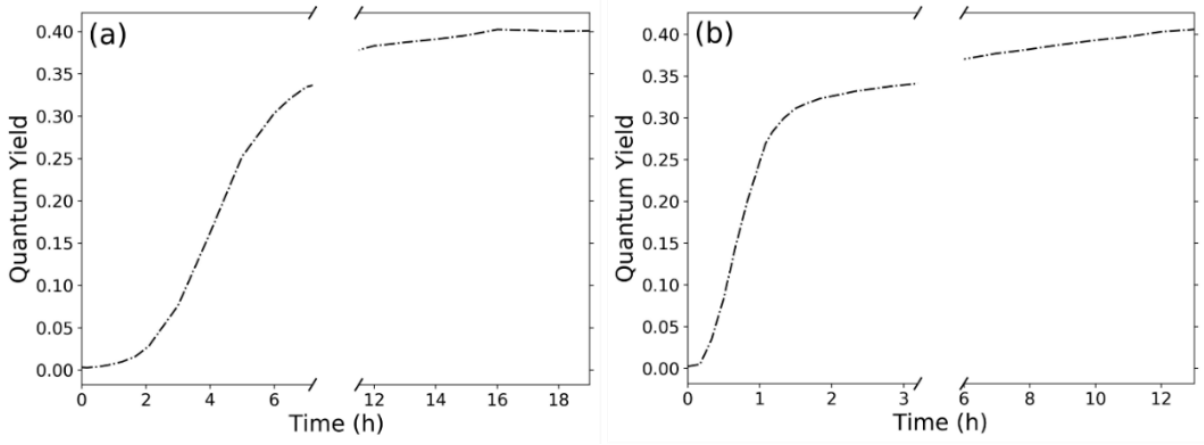

Figure 17. Φ dependence on **3a** crystallization time at RT
(a) without mechanical activation, (b) with mechanical activation.

It is clear from the Figure 17, that mechanical activation is significantly increasing the rate of crystallization, with mechanically activated sample restoring 75% of its original crystal state quantum yield just within an hour, while for naturally crystallizing samples, it takes about six times longer to reach the same quantum yield value.

To illustrate the effect of mechanical activation, pictures of activated crystallization process were taken with Keyence VHX-600 optical microscope (see Figure 18).

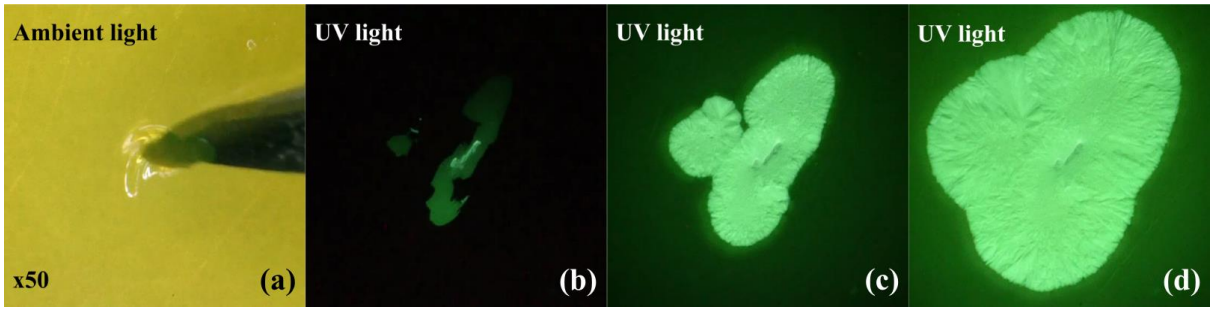

Figure 18. (a) mechanical activation of complex **3a** crystallization process, (b) start of crystallization, (c) 10 minutes after, and (d) 30 minutes after.

Next, the luminescence switchability of complex **3a** was demonstrated. To do that, the melting-crystallization cycle was repeated five times, with Φ being measured right after melting the sample and a day after (see Figure 19). Results show that the luminescence intensity of prepared material can be turned off by melting the material and then successfully restored by recrystallizing it.

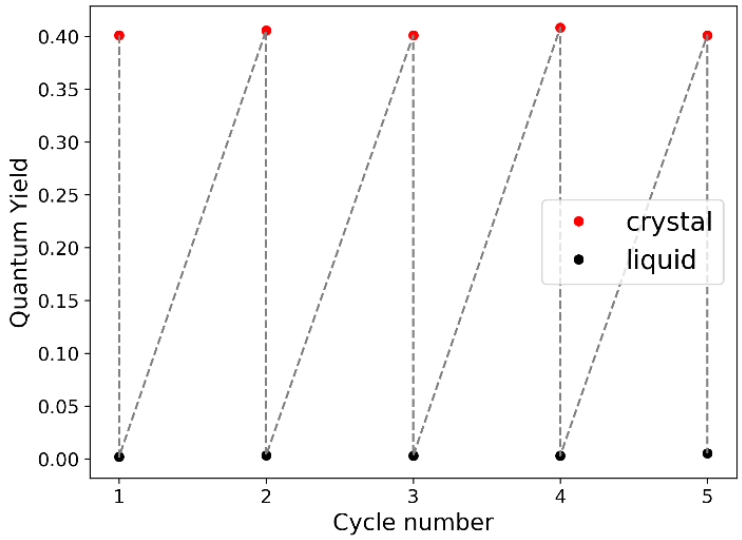

Figure 19. Melting-crystallization cycles of complex **3a**.

Luminescence temperature dependence and switchability demonstrated in Figure 16–Figure 19 are making complex **3a** a promising photoactive material, which can be implemented in various photochromic sensor systems.

3.4.2 $[P_{6,6,6,14}][Pt(PPy)Cl_2]$ as a light-emitting material

To demonstrate the applicability of complex **3a** as a light-emitting material, a thin luminescent film was prepared from the complex (see Figure 20 and Appendix 10).

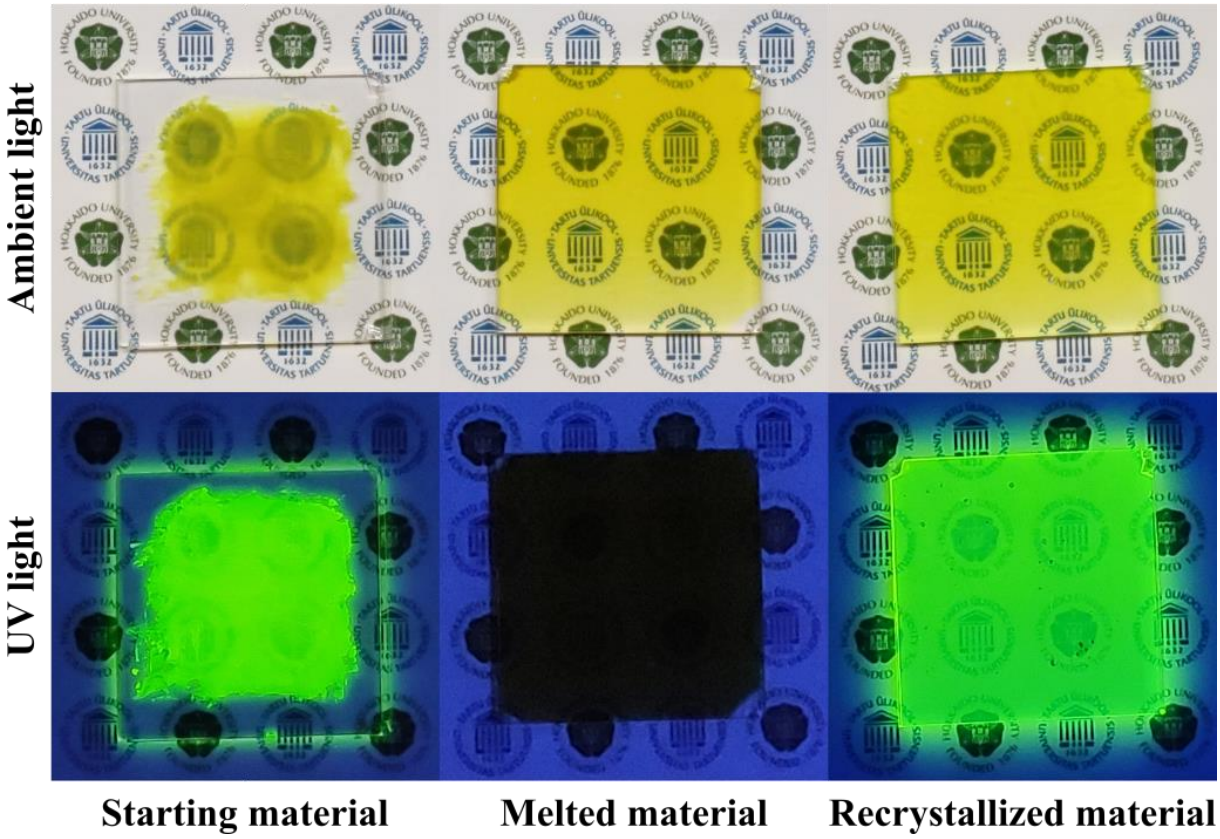

Figure 20. Preparation of thin luminescent film from complex **3a**.

As can be seen from Figure 20, the prepared material is non-luminescent at the liquid state and shows strong luminescence after recrystallization. Another important detail evident from the picture is that complex **3a**, when it is compressed into a thin film, is transparent at both liquid and crystal states, which is of high importance for light-emitting devices [3,5,7].

Bright luminescence and good film-forming capability of complex **3a** clearly demonstrated at Figure 20 prove that complex **3a** can be applied as an emitter in a new generation of displays.

SUMMARY

The current work aimed to prepare highly luminescent ionic liquids based on anionic platinum(II) complexes. Accordingly, a synthetic procedure was developed and optimized. In total, nine platinum complexes were synthesized, including three intermediate neutral complexes (**1**, **2a**–**2b**) and six target anionic complexes (**3a**–**3c** and **4a**–**4c**). Six out of nine synthesized complexes are previously unreported compounds (**2b**, **3a**–**3b,** and **4a**–**4c**). Structures of all synthesized complexes were confirmed by nuclear magnetic resonance spectroscopy. Within prepared novel anionic complexes, four were found to have a melting temperature below 100 °C and exhibited luminescence, which qualifies them as luminescent ionic liquids. Those complexes were:

- $[P_{6,6,6,14}][Pt(PPy)Cl_2]$ (**3a**)
- $[P_{6,6,6,14}][Pt(PPy)Br_2]$ (**4a**)
- [BMIm][Pt(PPy)Cl_2] (**3b**)
- [BMIm][Pt(PPy)Br_2] (**4b**)

For all six anionic complexes, luminescence emission and excitation spectra, as well as emission lifetime and absolute quantum yield, were measured at crystal state at 77 K and at room temperature. For **3a** and **4a,** luminescence measurements were also done at glass and liquid states. Among prepared LILs, **3a** exhibited the largest absolute quantum yield at room temperature (Φ = 0.40), which by far surpassed quantum yield values of similar LILs reported before. This result fulfilled the initial aim of the current work and prompted a further investigation of the photophysical properties of complex **3a**.

During the next research stage, the complex **3a** was studied in terms of its applicability in optoelectronic devices. First, its luminescence temperature dependence and switchability were reported, which gives rise to a possible application of **3a** in novel temperature measuring devices, such as luminescence thermometers and temperature threshold sensors.

Finally, to demonstrate the potential use of complex **3a** as an emitter in displays, the thin luminescent film was prepared out of it by recrystallization. Luminescence brightness and transparency of prepared film were then recorded via photography. High absolute luminescence quantum yield at room temperature, good film-forming capability, as well as transparency at both liquid and crystal states are making complex **3a** a promising material to be applied as the emitter in OLED and LEEC displays.

ACKNOWLEDGMENTS

The author would like to thank his supervisors Dr. Masaki Yoshida, Dr. Kaija Põhako-Esko, and Dr. Vladislav Ivaništšev, for their patience, support, and guidance during the preparation of the current study. The author would also like to thank all members of the Coordination Chemistry Laboratory of Hokkaido University for their help and support. Also, the Analysis Center of Hokkaido University for the elemental analysis measurements. Finally, Prof. Masako Kato, for her willingness to accept a short-term exchange student into her laboratory, for her wise guidance, and for providing all the materials and instrumentation used for the current study.

KOKKUVÕTE

21. sajandi esimesed kaks aastakümned arvatavasti jäävad ajalukku optoelektroonika valdkonna hüppelise arengu poolest, seda eelkõige uudsete sensorite ja ekraanide tehnoloogiate tõttu. Üks aktuaalsematest ja majanduslikult tähtsamatest trendidest antud valdkonnas on painutatavate ja rullitavate ekraanide valmistamine. Tänapäevaks on seda trendi toetanud maailma suurimad elektroonikaettevõtted, nagu LG, Samsung ja Apple [6,7] ning eksperdid ennustavad jätkuvat kapitali voolu ka tulevasel aastakümnel [7]. Mitmetest olemasolevatest tehnoloogiatest, uudsete ekraanide valmistamiseks sobivad kõige rohkem valgust kiirgavatel elektrokeemilistel elementidel (LEEC) või orgaanilistel valgusdioodidel (OLED) põhinevad seadmed [3,5,8,9].

Vaatamata LEEC ja OLED tehnoloogiate intensiivsele arengule, on neil siiamaani teatud puudusi, mis vajavad täiendamist. LEEC ja OLED seadmete keskne element on valgust kiirgav kiht, milleks on üldjuhul elektroluminestsentsest orgaanilisest ühendist tehtud õhuke kile [7]. Tänapäeva LEEC ja OLED ekraanides kasutusel olevate orgaaniliste ühendite suurimateks probleemideks on nende madal kvantsaagis, mis negatiivselt mõjub ekraanide heledusele [7], ja elektrokeemiline ebastabiilsus, mis vähendab ekraanide tööiga [6–8]. Nimetatud probleemide lahendamiseks otsitakse uusi tüüpe ühendeid valgust kiirgava kihi valmistamiseks ning erilist tähelepanu teadlaste poolt on saanud ioonsed vedelikud. Ioonsed vedelikud on tuntud nende laia elektrokeemilise akna ja termilise stabiilsuse poolest [13], kuid luminestsentsete ioonsete vedelike valmistamine on siiski jäänud väljakutset esitavaks alaks [11].

Luminestsentseid ioonseid vedelikke valmistatakse kombineerides metallikomplekse ja tavalisi ioonseid vedelikke, kusjuures kasutatakse nii haruldasi muldmetalle (eriti euroopiumi) [12,13,53], kui ka ülemineku metalle (nt vask, magneesium ja ruteenium) [14–16]. Kuigi praeguseks on sünteesitud mitmeid luminestsentseid ioonseid vedelikke, on neil kõigil ühine puudus: nende kvantsaagis toatemperatuuril on liiga väike [11]. Üks võimalustest selle probleemi lahendamiseks on kasutada luminestsentsete ioonsete vedelike valmistamiseks plaatina, mille kompleksid on tuntud oma ereda luminestsentsi poolest [10,11]. Luminestsentsete plaatina kompleksite valmistamisega ning nende uurimisega aktiivselt tegeleb Hokkaido Ülikooli koordinatsiooni keemia labor [10,11], mille juures on käesolev töö läbi viidud.

Antud töö oli ajendatud optoelektroonika aktuaalsusest ja majanduslikust perspektiivist. Läbiviidud uurimus keskendus luminestsentsete ioonsete vedelike valmistamisele

optoelektroonilisteks rakendusteks. Töö eesmärk oli sünteesida anioonsel plaatina(II) kompleksil põhinev luminestsentne ioonne vedelik, mille kvantsaagise väärtus toatemperatuuril oleks vähemalt 0,20.

Esimeses töö etapis arendati ja optimeeriti kahte sünteesirada, mille käigus valmistati üheksa plaatina kompleksi, sellehulgas kolm neutraalset vahekompleksi (**1**, **2a**–**2b**) ja kuus anioonset sihtkompleksi (**3a**–**3c** ja **4a**–**4c**). Sünteesitud kompleksitest kuus on varem avaldamata (**2b**, **3a**, **3b** ja **4a**–**4c**). Kõikide kompleksite struktuure kontrolliti tuumamagnetresonants-spektroskoopiaga. Seejärel mõõdeti valmistatud anioonsete kompleksite sulamistemperatuure ning leiti, et neljal oli sulamistemperatuur alla 100 °C, mis kvalifitseeris neid ioonsete vedelikena. Nendeks olid:

- $[P_{6,6,6,14}][Pt(PPy)Cl_2]$ (**3a**)
- $[P_{6,6,6,14}][Pt(PPy)Br_2]$ (**4a**)
- [BMIm][Pt(PPy)Cl_2] (**3b**)
- [BMIm][Pt(PPy)Br_2] (**4b**)

Töö teises etapis uuriti sünteesitud anioonsete kompleksite fotofüüsikalisi omadusi. Mõõdeti nende kristalloleku emissiooni- ja ergastusspektreid, kvantsaagis ja emissiooniaeg 77 K ja toatemperatuuri juures. $[P_{6,6,6,14}][Pt(PPy)Cl_2]$ (**3a**) ja $[P_{6,6,6,14}][Pt(PPy)Br_2]$ (**4a**) kompleksite puhul mõõtmisi teostati ka klaas- ja vedelolekus. Leiti, et sünteesitud kompleksite kvantsaagis ja emissiooniaeg sõltuvad temperatuurist, olles 77 K juures oluliselt suuremad kui toatemperatuuri juures. Lisaks sellele leiti, et $[Pt(PPy)Br_2]^-$ aniooniga kompleksite kvantsaagis on üldjuhul väiksem kui analoogsetel $[Pt(PPy)Cl_2]^-$ aniooniga kompleksitel. Broomi ligandi mõju kvantsaagisele võib selgitada broomi nõrgema ligandväljaga, mis soodustab mittekiirgusliku relaksatsiooni ning nõrgendab luminestsentsi. Seda oletust kinnitab fakt, et 77 K juures, kus mittekiirguslik relaksatsioon on suuremal määral maha surutud, kasvavad $[Pt(PPy)Br_2]^-$ aniooniga komplekside kvantsaagis ja emisiooniaeg oluliselt. Selleks, et tõestada halogeenide ligandvälja tugevuse mõju plaatina kompleksite emisiooni kvantsaagisele, võiks tulevikkus sünteesida ka $[Pt(PPy)I_2]^-$ aniooniga komplekse ning uurida nende luminestsentsomadusi.

Teistest keerulisem juhtum oli kompleksidega **3b** ja **4b**, kus ka kloori liganditega kompleksi **3b** kvantsaagis toatemperatuuril oli madal. Kompleksi **3b** puhul oletati, et madala kvantsaagise põhjuseks võiks olla $[BMIm]^+$ katiooni mittesümmeetrilisusest tingitud kristallstruktuuri

amorfsus. Selleks, et seda oletust kinnitada, võiks tulevikus komplekside **3b** ja **4b** kristallstruktuuri põhjalikumalt uurida röntgendifraktsiooni abil.

Sünteesitud ioonsete vedelike seas suurim kvantsaagis toatemperatuuril, Φ = 0,40, oli ühendil [$P_{6,6,6,14}$][Pt(PPy)Cl_2] (**3a**). Kvantsaagise väärtus 0,40 on peaaegu neli korda suurem varesemalt publitseeritud väärtustest [11], mis täies mahus rahuldas käesoleva töö eesmärgi. Ühendi [$P_{6,6,6,14}$][Pt(PPy)Cl_2] (**3a**) silmapaistva kvantsaagise ning madala sulamistemperatuuri (T_m = 50 °C) tõttu otsustati keskenduda viimases töö etapis just selle üksikasjalisele uurimisele.

Esimesena uuriti ühendi **3a** emissiooni sõltuvust temperatuurist, mõõtes emissioonispektrid temperatuuride vahemikus 25–55 °C. Leiti, et emissiooni intensiivsus langeb temperatuuri tõustes alguses suhteliselt aeglaselt, kuid 50 °C juures toimub järsk emissiooni intensiivsuse langus. See muutus on ootuspäraselt seotud ühendi sulamisega.

Seejärel uuriti ühendi **3a** tahke-vedelik ülemineku pöörduvust. Selle jaoks mõõdeti kompleksi kvantsaagist toatemperatuuril tahkes olekus (Φ = 0,40), siis sulatati seda ja mõõdeti kvantsaagist vedelas olekus (Φ < 0,01). Katset korrati viis korda näitamaks, et kummagi oleku kvantsaagis on püsiv ning valmistatud materjali luminestsentsi saab pöörduvalt kustutada (ehk saavutada nullilähedast kvantsaagist), viies kompleksi tahkest olekust vedelasse.

Lisaks mõõdeti ühendi **3a** kristallisatsiooni kiirust, jälgides kvantsaagise muutust ajas. Kristallisatsiooni uuriti kahel tingimusel: mehaanilise aktivatsiooniga (nõelaga torkamine) ja ilma selleta. Leiti, et tingimustest sõltumata kulub kompleksi **3a** täielikuks kristallisatsiooniks umbes 13-16 tundi, kuid mehaaniline aktiveerimine kiirendab oluliselt kristallisatsiooni algust.

Viimasena valmistati ühendist **3a** õhuke kile, et demonstreerida selle kasutatavust valgust kiirgava kihina OLED ja LEEC ekraanides. Valmistatud kile üles pildistamisega tõestati selle läbipaistvust tahkes olekus, mis on oluline parameeter OLED ja LEEC ekraanide valmistamisel [5]. Lisaks pildistati kompleksi **3a** temperatuurkontrolleriga mikroskoobi abil, et demonstreerida emissiooni klaasolekus. Klaasolek saavutati jahutades sulatatud kompleksi ülimadalala temperatuurini (−190 °C) vedelalämmastiku abil.

Sünteesitud ühend [$P_{6,6,6,14}$][Pt(PPy)Cl_2] (**3a**) on märkimisväärse kvantsaagise, temperatuurist sõltuva luminestsentsi ning kile moodustamise lihtsuse tõttu perspektiivne valgust kiirgav materjal. See võiks pakkuda huvi nii uudsete termosensorite kui ka ekraanide valmistajatele. Saadud materjali tutvustamiseks laiemale ringkonnale on tööle lisatud materjali luminestsentsomadusi demonstreeriv digitaalmeedia (vt Appendix 9 ja Appendix 10).

REFERENCES

[1] R. Gautier, C. Latouche, M. Paris, F. Massuyeau, Thermochromic Luminescent Materials and Multi-Emission Bands in d 10 Clusters, Sci. Rep. 7 (2017) 45537.

[2] Z. Zhang, J. Zhang, B. Wu, X. Li, Y. Chen, J. Huang, et al., Diarylethenes with a Narrow Singlet–Triplet Energy Gap Sensitizer: a Simple Strategy for Efficient Visible-Light Photochromism, Adv. Opt. Mater. 6 (2018) 1700847.

[3] P. Lundberg, Y. Tsuchiya, E.M. Lindh, S. Tang, C. Adachi, L. Edman, Thermally activated delayed fluorescence with 7% external quantum efficiency from a light-emitting electrochemical cell, Nat. Commun. 10 (2019) 5307.

[4] J. Liu, J. Wang, Z. Zhang, F. Molina-Lopez, G.-J.N. Wang, B.C. Schroeder, et al., Fully stretchable active-matrix organic light-emitting electrochemical cell array, Nat. Commun. 11 (2020) 3362.

[5] Y. Huang, E.-L. Hsiang, M.-Y. Deng, S.-T. Wu, Mini-LED, Micro-LED and OLED displays: present status and future perspectives, Light Sci. Appl. 9 (2020) 105.

[6] H.-W. Chen, J.-H. Lee, B.-Y. Lin, S. Chen, S.-T. Wu, Liquid crystal display and organic light-emitting diode display: present status and future perspectives, Light Sci. Appl. 7 (2018) 17168–17168.

[7] G. Hong, X. Gan, C. Leonhardt, Z. Zhang, J. Seibert, J.M. Busch, et al., A Brief History of OLEDs—Emitter Development and Industry Milestones, Adv. Mater. n/a (n.d.) 2005630.

[8] C. Keum, C. Murawski, E. Archer, S. Kwon, A. Mischok, M.C. Gather, A substrateless, flexible, and water-resistant organic light-emitting diode, Nat. Commun. 11 (2020) 6250.

[9] Y. Luo, S. Li, Y. Zhao, C. Li, Z. Pang, Y. Huang, et al., An Ultraviolet Thermally Activated Delayed Fluorescence OLED with Total External Quantum Efficiency over 9%, Adv. Mater. 32 (2020) 2001248.

[10] T. Ogawa, M. Yoshida, H. Ohara, A. Kobayashi, M. Kato, A dual-emissive ionic liquid based on an anionic platinum(II) complex, Chem. Commun. 51 (2015) 13377–13380.

[11] T. Ogawa, W.M.C. Sameera, M. Yoshida, A. Kobayashi, M. Kato, Luminescent ionic liquids based on cyclometalated platinum(II) complexes exhibiting thermochromic behaviour in different colour regions, Dalton Trans. 47 (2018) 5589–5594.

[12] D. Yang, Y. Xu, Y. Yao, J. Zhang, J. Wang, Y. Wang, A red light-emitting ionic europium (III) complex applied in near UV LED, Synth. Met. 221 (2016) 236–241.

[13] S. Tang, A. Babai, A.-V. Mudring, Europium-Based Ionic Liquids as Luminescent Soft Materials, Angew. Chem. Int. Ed. 47 (2008) 7631–7634.

[14] S. Gago, L. Cabrita, J.C. Lima, L.C. Branco, F. Pina, Synthesis and characterization of luminescent room temperature ionic liquids based on Ru(bpy)(CN)42−, Dalton Trans. 42 (2013) 6213–6218.

[15] S. Pitula, A.-V. Mudring, Synthesis, Structure, and Physico-optical Properties of Manganate(II)-Based Ionic Liquids, Chem. – Eur. J. 16 (2010) 3355–3365.

[16] E.T. Spielberg, E. Edengeiser, B. Mallick, M. Havenith, A.-V. Mudring, (1-Butyl-4-methyl-pyridinium)[Cu(SCN)2]: A Coordination Polymer and Ionic Liquid, Chem. – Eur. J. 20 (2014) 5338–5345.

[17] N. Zhou, Y. Zhang, Z. Chen, X. Zhu, X. He, Developing luminescent ratiometric thermometers based on copolymers containing Platinum(II) isocyanide complex, Dyes Pigments. 184 (2021) 108815.

[18] X. Rao, T. Song, J. Gao, Y. Cui, Y. Yang, C. Wu, et al., A Highly Sensitive Mixed Lanthanide Metal–Organic Framework Self-Calibrated Luminescent Thermometer, J. Am. Chem. Soc. 135 (2013) 15559–15564.

[19] Y. Cui, H. Xu, Y. Yue, Z. Guo, J. Yu, Z. Chen, et al., A Luminescent Mixed-Lanthanide Metal–Organic Framework Thermometer, J. Am. Chem. Soc. 134 (2012) 3979–3982.

[20] X. Chen, Z. Zheng, L. Teng, R. Wei, F. Hu, H. Guo, Self-calibrated optical thermometer based on luminescence from SrLu2O4:Bi3+,Eu3+ phosphors, RSC Adv. 8 (2018) 35422–35428.
[21] L. Chen, K. He, G. Bai, H. Xie, X. Yang, S. Xu, Non-contact luminescence thermometer based on upconversion emissions from Er3+-doped beta-Ga2O3 with wide bandgap, J. Alloys Compd. 846 (2020) 156425.
[22] C.D.S. Brites, P.P. Lima, N.J.O. Silva, A. Millán, V.S. Amaral, F. Palacio, et al., A Luminescent Molecular Thermometer for Long-Term Absolute Temperature Measurements at the Nanoscale, Adv. Mater. 22 (2010) 4499–4504.
[23] B. Valeur, M.N. Berberan-Santos, A Brief History of Fluorescence and Phosphorescence before the Emergence of Quantum Theory, J. Chem. Educ. 88 (2011) 731–738.
[24] M.Y. Berezin, S. Achilefu, Fluorescence Lifetime Measurements and Biological Imaging, Chem. Rev. 110 (2010) 2641–2684.
[25] C. Ronda, Luminescence: From Theory to Applications, 2007.
[26] J.R. Lakowicz, Principles of Fluorescence Spectroscopy, Springer US, Boston, MA, 2006, pp. 1–26.
[27] C. Würth, D. Geißler, T. Behnke, M. Kaiser, U. Resch-Genger, Critical review of the determination of photoluminescence quantum yields of luminescent reporters, Anal. Bioanal. Chem. 407 (2015) 59–78.
[28] J.-R. Albani, Structure and Dynamics of Macromolecules: Absorption and Fluorescence Studies, 2004.
[29] J.R. Lakowicz, Principles of Fluorescence Spectroscopy, Springer US, Boston, MA, 2006, pp. 27–61.
[30] J. Włodarczyk, B. Kierdaszuk, Interpretation of Fluorescence Decays using a Power-like Model, Biophys. J. 85 (2003) 589–598.
[31] C. Würth, J. Pauli, C. Lochmann, M. Spieles, U. Resch-Genger, Integrating Sphere Setup for the Traceable Measurement of Absolute Photoluminescence Quantum Yields in the Near Infrared, Anal. Chem. 84 (2012) 1345–1352.
[32] T.-S. Ahn, R.O. Al-Kaysi, A.M. Müller, K.M. Wentz, C.J. Bardeen, Self-absorption correction for solid-state photoluminescence quantum yields obtained from integrating sphere measurements, Rev. Sci. Instrum. 78 (2007) 086105.
[33] L. Troy, K. McFarland, S. Littman-Power, B.J. Kelly, E.T. Walpole, D. Wyld, et al., Cisplatin-based therapy: a neurological and neuropsychological review, Psychooncology. 9 (2000) 29–39.
[34] J.A. Gareth Williams, S. Develay, D.L. Rochester, L. Murphy, Optimising the luminescence of platinum(II) complexes and their application in organic light emitting devices (OLEDs), Coord. Chem. Rev. 252 (2008) 2596–2611.
[35] C.A. Craig, F.O. Garces, R.J. Watts, R. Palmans, A.J. Frank, Luminescence properties of two new Pt(II)-2-phenylpyridine complexes; the influence of metal-carbon bonds, Coord. Chem. Rev. 97 (1990) 193–208.
[36] F. Barigelletti, D. Sandrini, M. Maestri, V. Balzani, A. Von Zelewsky, L. Chassot, et al., Temperature dependence of the luminescence of cyclometalated palladium(II), rhodium(III), platinum(II), and platinum(IV) complexes, Inorg. Chem. 27 (1988) 3644–3647.
[37] L. Chassot, A. Von Zelewsky, D. Sandrini, M. Maestri, V. Balzani, Photochemical preparation of luminescent platinum(IV) complexes via oxidative addition on luminescent platinum(II) complexes, J. Am. Chem. Soc. 108 (1986) 6084–6085.
[38] D.J. Mabbott, B.E. Mann, P.M. Maitlis, Cationic (η3-allylic)(η4-diene)-palladium and -platinum complexes, J. Chem. Soc. Dalton Trans. (1977) 294–299.

[39] P.-I. Kvam, J. Songstad, J.C. Hanson, J. Songstad, C. Lundberg, J. Arnarp, et al., Preparation and Characterization of Some Cyclometalated Pt(II) Complexes from 2-Phenylpyridine and 2-(2'-Thienyl)pyridine., Acta Chem. Scand. 49 (1995) 313–324.
[40] L. Chassot, E. Mueller, A. Von Zelewsky, cis-Bis(2-phenylpyridine)platinum(II) (CBPPP): a simple molecular platinum compound, Inorg. Chem. 23 (1984) 4249–4253.
[41] L. Ricciardi, M.L. Deda, A. Ionescu, N. Godbert, I. Aiello, M. Ghedini, Anionic cyclometallated Pt(II) square-planar complexes: new sets of highly luminescent compounds, Dalton Trans. 46 (2017) 12625–12635.
[42] R.C. Evans, P. Douglas, C.J. Winscom, Coordination complexes exhibiting room-temperature phosphorescence: Evaluation of their suitability as triplet emitters in organic light emitting diodes, Coord. Chem. Rev. 250 (2006) 2093–2126.
[43] M. Yoshida, M. Kato, Cation-controlled luminescence behavior of anionic cyclometalated platinum(II) complexes, Coord. Chem. Rev. 408 (2020) 213194.
[44] T. Ogawa, W.M.C. Sameera, M. Yoshida, A. Kobayashi, M. Kato, Phosphorescence properties of anionic cyclometalated platinum(II) complexes with fluorine-substituted tridentate diphenylpyridine in the solid state, Chem. Phys. Lett. 739 (2020) 137024.
[45] K. Li, G.S.M. Tong, J. Yuan, C. Ma, L. Du, C. Yang, et al., Excitation-Wavelength-Dependent and Auxiliary-Ligand-Tuned Intersystem-Crossing Efficiency in Cyclometalated Platinum(II) Complexes: Spectroscopic and Theoretical Studies, Inorg. Chem. 59 (2020) 14654–14665.
[46] D. Wang, X. Chen, H. Yang, D. Zhong, B. Liu, X. Yang, et al., The synthesis of cyclometalated platinum(ii) complexes with benzoaryl-pyridines as C^N ligands for investigating their photophysical, electrochemical and electroluminescent properties, Dalton Trans. 49 (2020) 15633–15645.
[47] P. Wasserscheid, W. Keim, Ionic Liquids—New "Solutions" for Transition Metal Catalysis, Angew. Chem. Int. Ed. 39 (2000) 3772–3789.
[48] K.J. Fraser, D.R. MacFarlane, Phosphonium-Based Ionic Liquids: An Overview, Aust. J. Chem. 62 (2009) 309–321.
[49] T.P. Thuy Pham, C.-W. Cho, Y.-S. Yun, Environmental fate and toxicity of ionic liquids: A review, Water Res. 44 (2010) 352–372.
[50] E. Jónsson, Ionic liquids as electrolytes for energy storage applications – A modelling perspective, Energy Storage Mater. 25 (2020) 827–835.
[51] P. Nockemann, E. Beurer, K. Driesen, R.V. Deun, K.V. Hecke, L.V. Meervelt, et al., Photostability of a highly luminescent europium β-diketonate complex in imidazolium ionic liquids, Chem. Commun. 0 (2005) 4354–4356.
[52] E. Guillet, D. Imbert, R. Scopelliti, J.-C.G. Bünzli, Tuning the Emission Color of Europium-Containing Ionic Liquid-Crystalline Phases, Chem. Mater. 16 (2004) 4063–4070.
[53] Y. Mei, B. Yan, White luminescent hybrid soft materials of lanthanide (Eu3+, Sm3+) beta-diketonates and Ag/Ag2S nanoparticles based with thiol-functionalized ionic liquid bridge, Inorg. Chem. Commun. 40 (2014) 39–42.
[54] K. Driesen, P. Nockemann, K. Binnemans, Ionic liquids as solvents for near-infrared emitting lanthanide complexes, Chem. Phys. Lett. 395 (2004) 306–310.
[55] A. Tokarev, J. Larionova, Y. Guari, C. Guérin, J.M. López-de-Luzuriaga, M. Monge, et al., Gold- and silver-based ionic liquids: modulation of luminescence depending on the physical state, Dalton Trans. 39 (2010) 10574–10576.
[56] Y. Yoshida, J. Fujii, G. Saito, T. Hiramatsu, N. Sato, Dicyanoaurate(I) salts with 1-alkyl-3-methylimidazolium: luminescent properties and room-temperature liquid forming, J. Mater. Chem. 16 (2006) 724–727.

[57] M. Maestri, C. Deuschel-Cornioley, A. von Zelewsky, Spectroscopic properties of Pt(II) and Pd(II) complexes with aromatic terdendate (C″>N^C) cyclometallating ligands, Coord. Chem. Rev. 111 (1991) 117–123.
[58] H.L. Ngo, K. LeCompte, L. Hargens, A.B. McEwen, Thermal properties of imidazolium ionic liquids, Thermochim. Acta. 357–358 (2000) 97–102.
[59] N. Calvar, E. Gómez, E.A. Macedo, Á. Domínguez, Thermal analysis and heat capacities of pyridinium and imidazolium ionic liquids, Thermochim. Acta. 565 (2013) 178–182.
[60] S.P. Verevkin, V.N. Emel'yanenko, D.H. Zaitsau, R.V. Ralys, C. Schick, Ionic Liquids: Differential Scanning Calorimetry as a New Indirect Method for Determination of Vaporization Enthalpies, J. Phys. Chem. B. 116 (2012) 4276–4285.
[61] A. Diedrichs, J. Gmehling, Measurement of heat capacities of ionic liquids by differential scanning calorimetry, Fluid Phase Equilibria. 244 (2006) 68–77.
[62] G. Höhne, W.F. Hemminger, H.-J. Flammersheim, Differential Scanning Calorimetry, 2nd ed., Springer-Verlag, Berlin Heidelberg, 2003.
[63] A.W. Coats, J.P. Redfern, Thermogravimetric analysis. A review, Analyst. 88 (1963) 906–924.
[64] A. König, M. Stepanski, A. Kuszlik, P. Keil, C. Weller, Ultra-purification of ionic liquids by melt crystallization, Chem. Eng. Res. Des. 86 (2008) 775–780.
[65] Y. Cao, T. Mu, Comprehensive Investigation on the Thermal Stability of 66 Ionic Liquids by Thermogravimetric Analysis, Ind. Eng. Chem. Res. 53 (2014) 8651–8664.
[66] B.E. Mann, B.L. Shaw, G. Shaw, Transition metal–carbon bonds. Part XXVI. Allylic and olefin complexes of platinum(II), J. Chem. Soc. Inorg. Phys. Theor. (1971) 3536–3544.
[67] M.J. Romero, A. Rodríguez, A. Fernández, M. López-Torres, D. Vázquez-García, J.M. Vila, et al., Crystal packing in a solvent-free or chloroform-solvated dinuclear platinum(III) organometallic complex, Polyhedron. 30 (2011) 2444–2450.
[68] S. Fuertes, H. García, M. Perálvarez, W. Hertog, J. Carreras, V. Sicilia, Stepwise Strategy to Cyclometallated PtII Complexes with N-Heterocyclic Carbene Ligands: A Luminescence Study on New β-Diketonate Complexes, Chem. – Eur. J. 21 (2015) 1620–1631.
[69] L. Cammarata, S.G. Kazarian, P.A. Salter, T. Welton, Molecular states of water in room temperature ionic liquids, Phys. Chem. Chem. Phys. 3 (2001) 5192–5200.
[70] K. Wippermann, J. Giffin, C. Korte, In Situ Determination of the Water Content of Ionic Liquids, J. Electrochem. Soc. 165 (2018) H263.
[71] D. Black, G. Deacon, G. Edwards, Observations on the Mechanism of Halogen-Bridge Cleavage by Unidentate Ligands in Square Planar Palladium and Platinum Complexes, Aust. J. Chem. 47 (1994) 217.
[72] W.R. Dawson, M.W. Windsor, Fluorescence yields of aromatic compounds, J. Phys. Chem. 72 (1968) 3251–3260.
[73] T. Sajoto, P.I. Djurovich, A.B. Tamayo, J. Oxgaard, W.A. Goddard, M.E. Thompson, Temperature Dependence of Blue Phosphorescent Cyclometalated Ir(III) Complexes, J. Am. Chem. Soc. 131 (2009) 9813–9822.
[74] X. Zhou, P.L. Burn, B.J. Powell, Bond Fission and Non-Radiative Decay in Iridium(III) Complexes, Inorg. Chem. 55 (2016) 5266–5273.
[75] W. Shen, W. Zhang, C. Zhu, Theoretical study of the substituent effect controlling the radiative and non-radiative decay processes of platinum(II) complexes, Phys. Chem. Chem. Phys. 19 (2017) 23532–23540.
[76] D.K. Singh, S. Cha, D. Nam, H. Cheong, S.-W. Joo, D. Kim, Raman Spectroscopic Study on Alkyl Chain Conformation in 1-Butyl-3-methylimidazolium Ionic Liquids and their Aqueous Mixtures, ChemPhysChem. 17 (2016) 3040–3046.

[77] V. Morad, I. Cherniukh, L. Pöttschacher, Y. Shynkarenko, S. Yakunin, M.V. Kovalenko, Manganese(II) in Tetrahedral Halide Environment: Factors Governing Bright Green Luminescence, Chem. Mater. 31 (2019) 10161–10169.
[78] P. Marć, N. Przybysz, A. Molska, L.R. Jaroszewicz, Photonic Crystal Fiber Transducers for an Optical Fiber Multilevel Temperature Threshold Sensor, J. Light. Technol. 36 (2018) 898–903.
[79] S. Kang, H. Choi, S. Park, C. Park, J. Lee, U. Lee, et al., Fire in Your Hands: Understanding Thermal Behavior of Smartphones, 25th Annu. Int. Conf. Mob. Comput. Netw., Association for Computing Machinery (2019) 1–16.

APPENDICES

Appendix 1. Reagents, materials, and solvents used.

3-chloro-2-methyl-1-propene (98.0% purity), 2-phenylpyridine (98.0% purity), [BMIm]Cl (98.0% purity) and [BMIm]Br (98.0% purity) were purchased from Tokyo Chemical Industry Co., Ltd.

[TBA]Cl (98.0% purity), [TBA]Br (98.0% purity) and LiBr (99.5% purity) were purchased from FUJIFILM Wako Pure Chemical Co.

K_2PtCl_4 (98% purity), $[P_{6,6,6,14}]Cl$ (95.0% purity) and $[P_{6,6,6,14}]Br$ (95.0% purity) were purchased from Aldrich Chemical Co., Inc.

All solvents and molecular sieves were purchased from Kanto Chemical Co., Inc.

Appendix 2. Structures of target Pt(II) complexes.

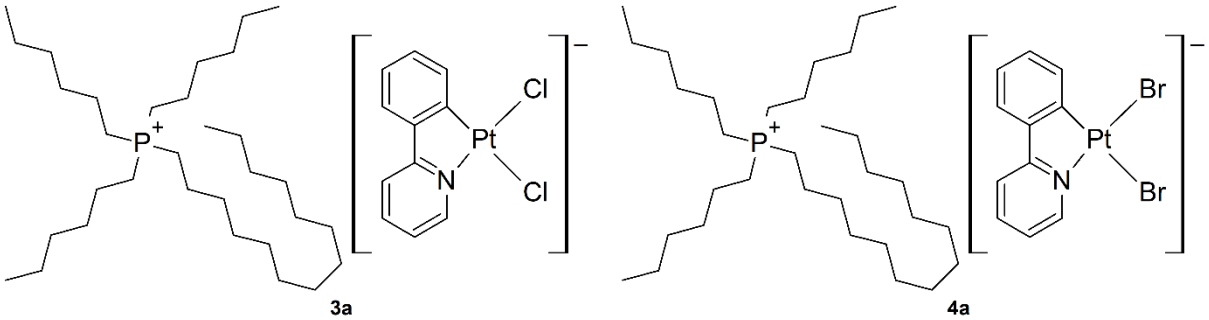

3a 4a

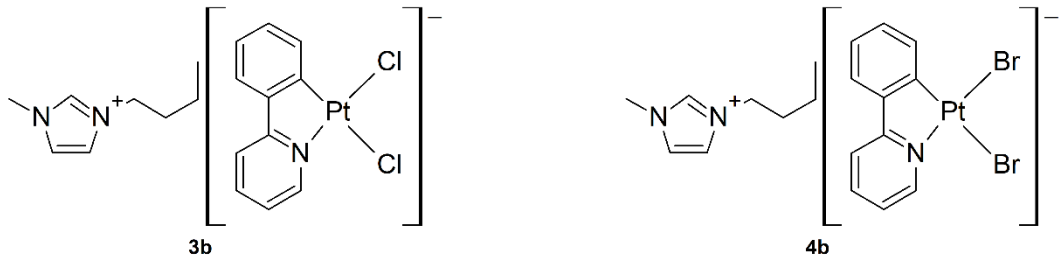

3b 4b

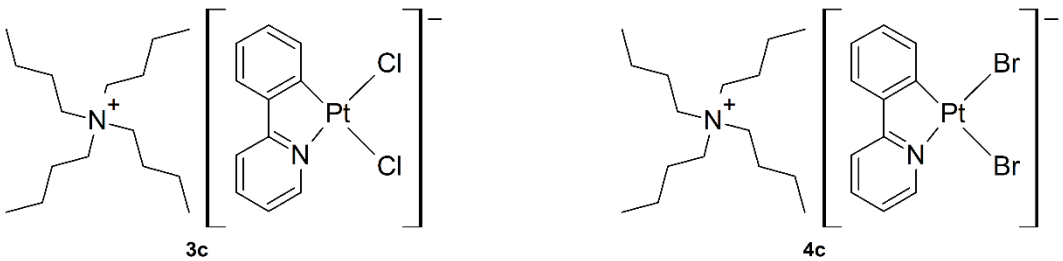

3c 4c

Appendix 3. ^{1}H NMR spectra of complexes **1**, **2a**–**2b** and **3a**.

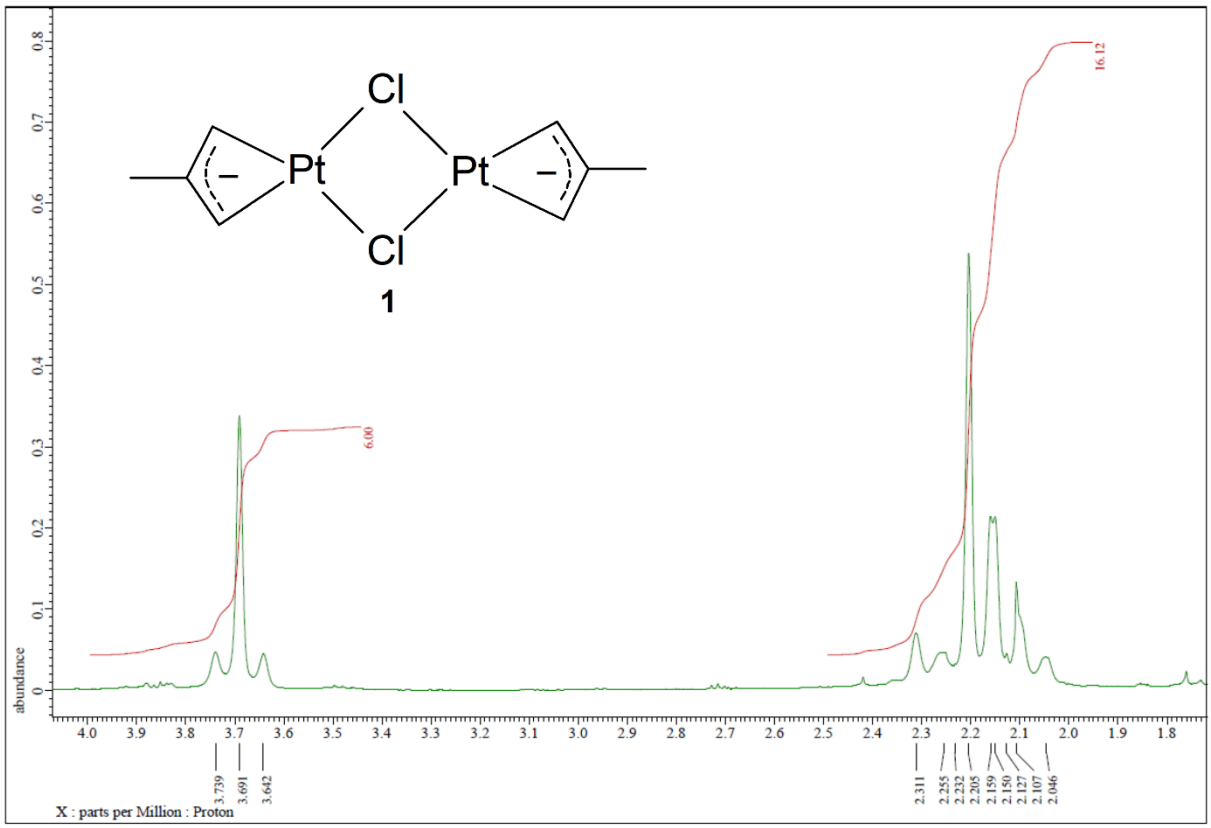

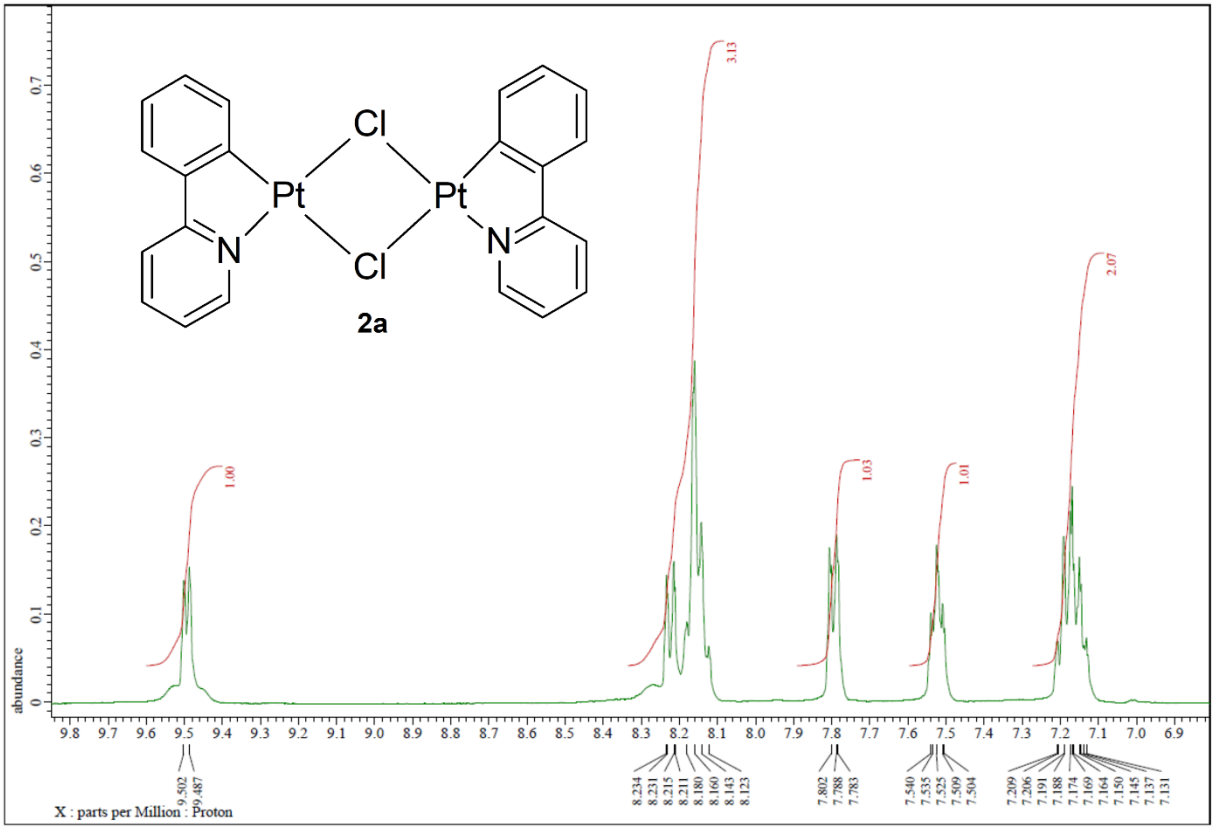

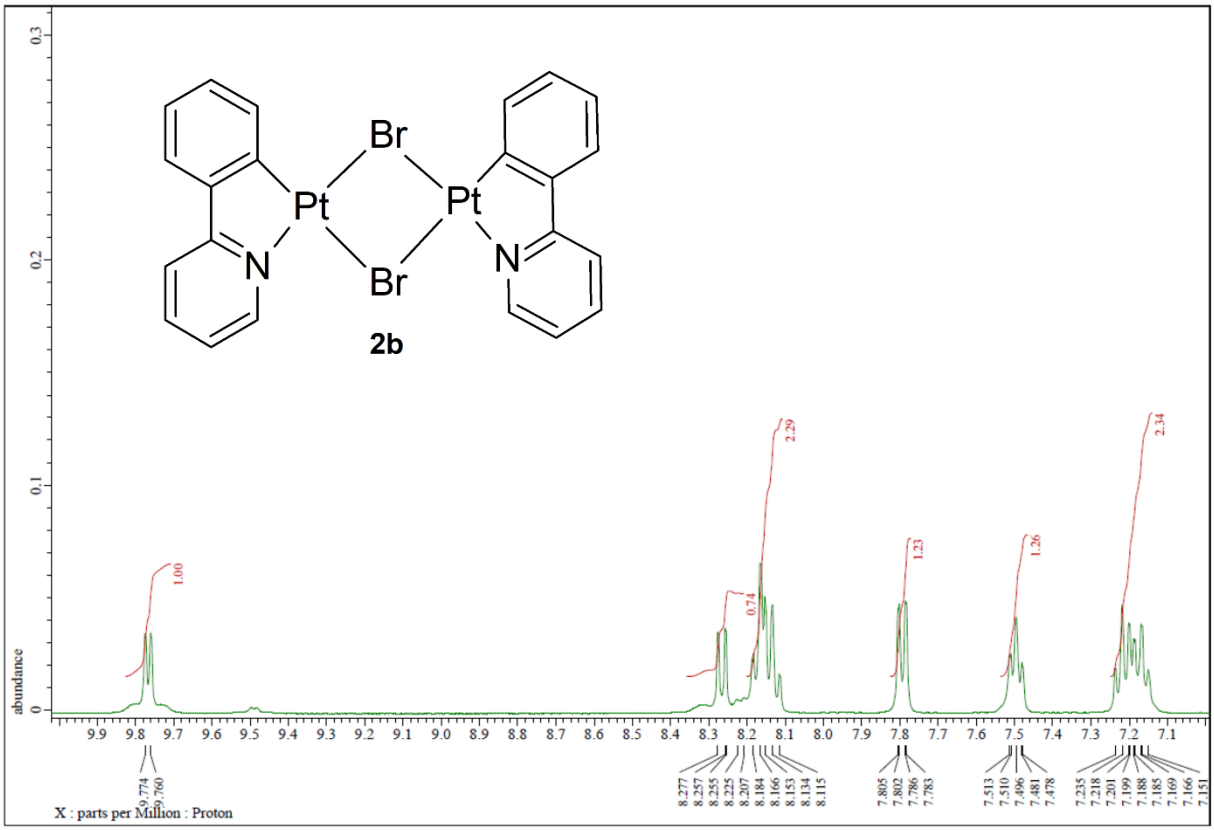
Br
Pt
Pt
N
N
Br
2b
abundance
X : parts per Million : Proton

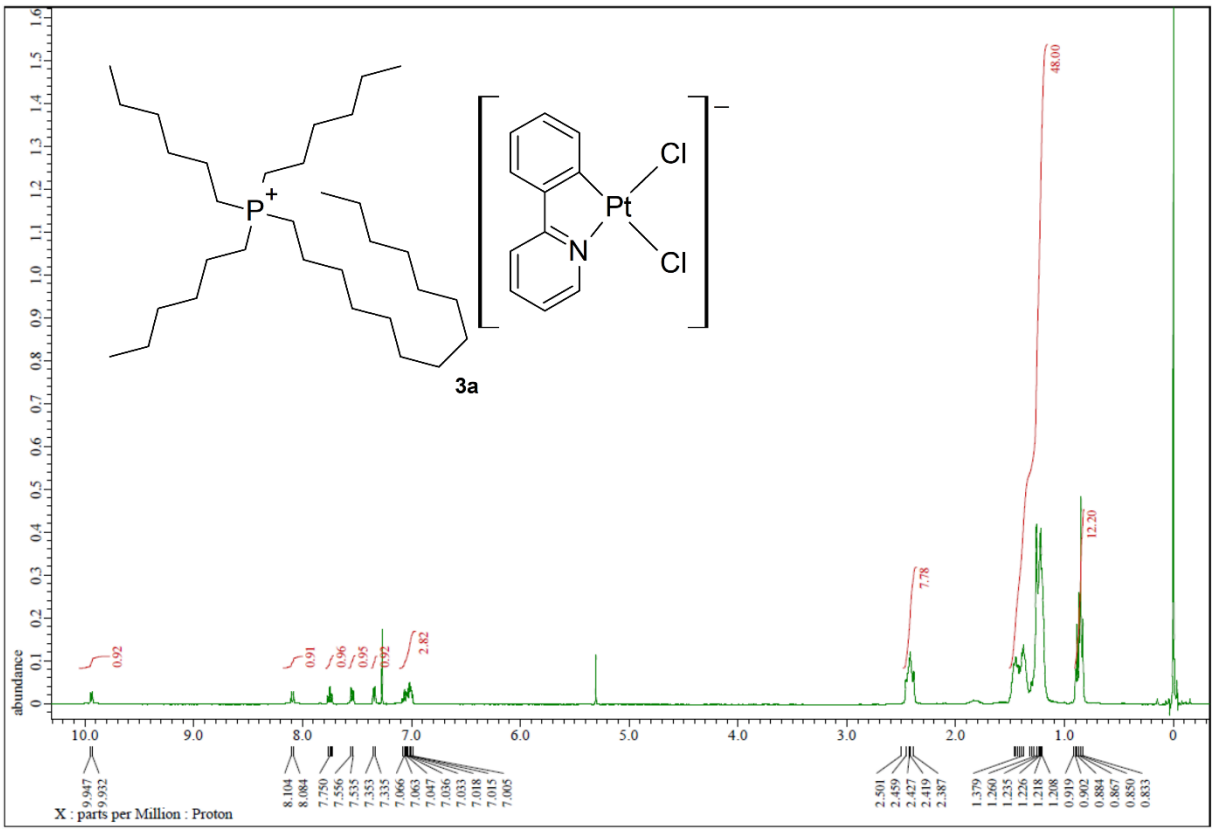
P+
Pt
Cl
Cl
N
3a
abundance
X : parts per Million : Proton

Appendix 4. Synthesis scheme for complex **3a**.

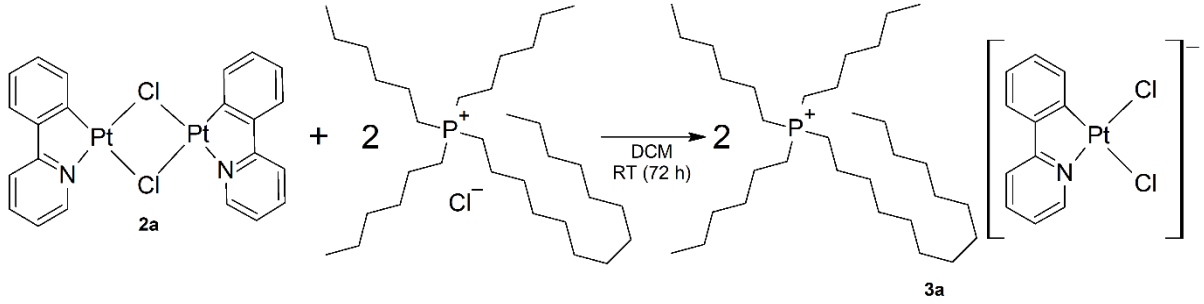

Appendix 5. Details of syntheses for complexes **3a**–**3b**, **4a**–**4c**.

Complex, Formula	*M* (g/mol)	Dimer[a]		Salt[b]		Product		Yield (%)
		m (mg)	*n* (mmol)	*m* (mg)	*n* (mmol)	*m* (mg)	*n* (mmol)	
$[P_{6,6,6,14}]$ $[Pt(PPy)Cl_2]$ (**3a**)	904.04	73.6	0.10	99.6	0.19	172.8	0.19	100
[BMIm] $[Pt(PPy)Cl_2]$ (**3b**)	559.40	79.9	0.10	36.5	0.21	116.4	0.21	98
		53.7	0.07	25.8	0.15	77.5	0.14	99
$[P_{6,6,6,14}]$ $[Pt(PPy)Br_2]$ (**4a**)	992.94	77.9	0.09	106	0.19	175.4	0.18	97
[BMIm] $[Pt(PPy)Br_2]$ (**4b**)	648.30	61.4	0.07	33.7	0.15	90.8	0.14	98
		54.4	0.06	28	0.13	76.4	0.12	93
[TBA] $[Pt(PPy)Br_2]$ (**4c**)	751.55	60.8	0.07	45.5	0.14	104.4	0.14	98
		96.3	0.11	72.1	0.22	166.2	0.22	99

[a]Dimer: **2a** or **2b** accordingly. [b]Salt: [Cat][Hal] (see Figure 8).

Appendix 6. ^{1}H NMR and elemental analysis results for complexes **3b** and **4a**–**4c**.

[BMIm][Pt(PPy)Cl_2] (**3b**):

^{1}H NMR (chloroform-d, 400 MHz) δ 10.21 (s, 1H), 9.80 (dd, *J* = 5.9, 1.1 Hz, 1H), 8.01 (dd, *J* = 7.6, 1.4 Hz, 1H), 7.77 (td, *J* = 7.7, 1.4 Hz, 1H), 7.57 (d, *J* = 7.6 Hz, 1H), 7.35 (dd, *J* = 7.5, 1.2 Hz, 1H), 7.23 (t, *J* = 1.8 Hz, 1H), 7.18 (t, *J* = 1.8 Hz, 1H), 7.09-7.00 (m, 3H), 4.24 (t, *J* = 7.5 Hz, 2H), 4.02 (s, 3H), 1.80-1.73 (m, 2H), 1.22 (sext, *J* = 7.5 Hz, 2H), 0.81 (t, *J* = 7.4 Hz, 3H) ppm.

After purification with diethyl ether, results of elemental analysis were in perfect agreement with calculated atomic composition of [BMIm][Pt(PPy)Cl_2]: C, 40.78%; H, 4.16%; N, 7.38% (found) and C, 40.80%; H, 4.14%; N, 7.51% (calculated).

[$P_{6,6,6,14}$][Pt(PPy)Br_2] (**4a**):

^{1}H NMR (chloroform-d, 400 MHz) δ 10.17 (dd, *J* = 6.0, 1.0 Hz, 1H), 8.33 (dd, *J* = 7.1, 2.0 Hz, 1H), 7.75 (td, *J* = 7.7, 1.4 Hz, 1H), 7.55 (d, *J* = 7.6 Hz, 1H), 7.33 (dd, *J* = 7.0, 2.2 Hz, 1H), 7.06-6.99 (m, 3H), 2.41 (m, 8H), 1.47-1.21 (m, 48H), 0.87 (m, 12H) ppm.

Elemental analysis showed only some leftovers of hexane, which was used for washing: C, 52.77%; H, 8.06%; N, 1.28% (found) and C, 52.82%; H, 7.93%; N, 1.37% (calculated for [$P_{6,6,6,14}$][Pt(PPy)Br_2]·0.3 hexane).

[BMIm][Pt(PPy)Br_2] (**4b**):

^{1}H NMR (chloroform-d, 400 MHz) δ 10.11 (s, 1H), 10.04 (dd, *J* = 5.9, 1.0 Hz, 1H), 8.25 (dd, *J* = 6.9, 2.1 Hz, 1H), 7.79 (td, *J* = 7.7, 1.5 Hz, 1H), 7.59 (d, *J* = 7.4 Hz, 1H), 7.36 (dd, *J* = 6.8, 2.3 Hz, 1H), 7.23 (m, 1H), 7.18 (m 1H), 7.07-7.03 (m, 3H), 4.22 (t, *J* = 4.3 Hz, 2H), 4.00 (s, 3H), 1.80-1.73 (m, 2H), 1.22 (sext, *J* = 4.3 Hz, 2H), 0.82 (t, *J* = 4.3 Hz, 3H) ppm.

Results of elemental analysis were almost identical to the calculated atomic composition of [BMIm][Pt(PPy)Br_2]: C, 35.20%; H, 3.58%; N, 6.48% (found) and C, 35.26%; H, 3.58%, N, 6.45% (calculated).

[TBA][Pt(PPy)Br_2] (**4c**):

^{1}H NMR (chloroform-d, 400 MHz) δ 10.16 (dd, *J* = 5.9, 1.0 Hz, 1H), 8.32 (dd, *J* = 6.7, 2.3 Hz, 1H), 7.76 (td, *J* = 7.7, 1.4 Hz, 1H), 7.55 (d, *J* = 7.8 Hz, 1H), 7.33 (dd, *J* = 6.5, 2.6 Hz, 1H), 7.03-6.99 (m, 3H), 3.29 (m, 8H), 1.57-1.50 (m, 8H), 1.36-1.27 (m, 8H), 0.87 (t, 12H, *J* = 7.3 Hz, 12H) ppm.

Results of elemental analysis were in perfect agreement to the calculated atomic composition of [TBA][Pt(PPy)Br_2]: C, 43.15%; H, 5.905; N, 3.73% (found) and C, 43.04%; H, 5.89%; N, 3.64% (calculated).

Appendix 7. Synthesis route for complex **3c**.

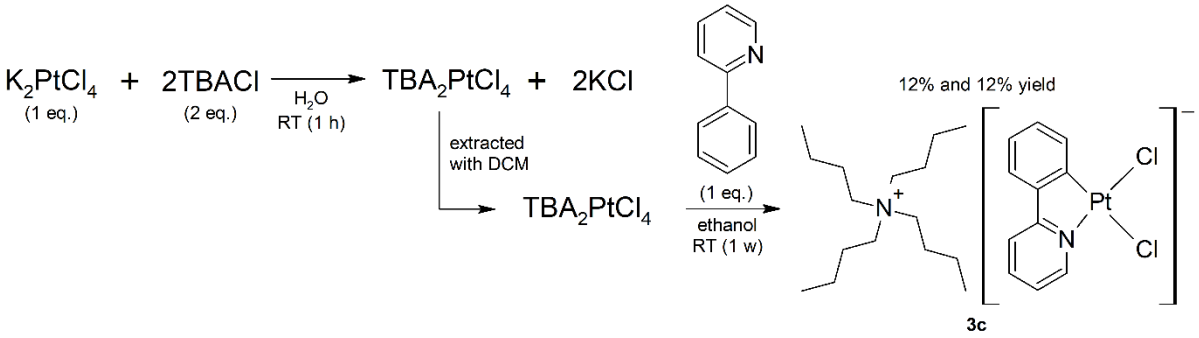

To prepare complex **3c** first cation exchange reaction was conducted by mixing 0.4682 g (1.1 mmol) of K_2PtCl_4 and 0.6306 g (2.3 mmol) of tetrabutylammonium chloride in 56 mL of deionized water for one hour at RT. Resulting solution was then extracted with DCM (once with 20 ml and twice with 15 mL), organic phase separated and concentrated on rotary evaporator. Obtained TBA_2PtCl_4 was then dissolved in 225 mL of ethanol, 180 µL (1.1 mmol) of 2-phenylpyridine added and mixture was stirred for one week at RT. After that, solution was centrifugated to remove formed crude Pt powder and concentrated on rotary evaporator until some of the crystals precipitated. Then concentrated solution of about 20 mL was left over weekend for slow crystallization. Formed crystals were then filtered, washed thrice with 5 mL of diethyl ether and dried overnight *in vacuo*. Finally, 88.6 mg (12% yield) of neon yellow crystals with a bright green luminescence at RT, [TBA][Pt(PPy)Cl_2] (**3c**), were obtained. The ^{1}H NMR spectrum was identical to the published one [35].

Same synthesis route, but at a double scale, was later repeated to result in 197,6 mg (12% yield) of neat complex **3c**.

Appendix 8. DSC curves for complexes **4a, 3b** and **4b**.

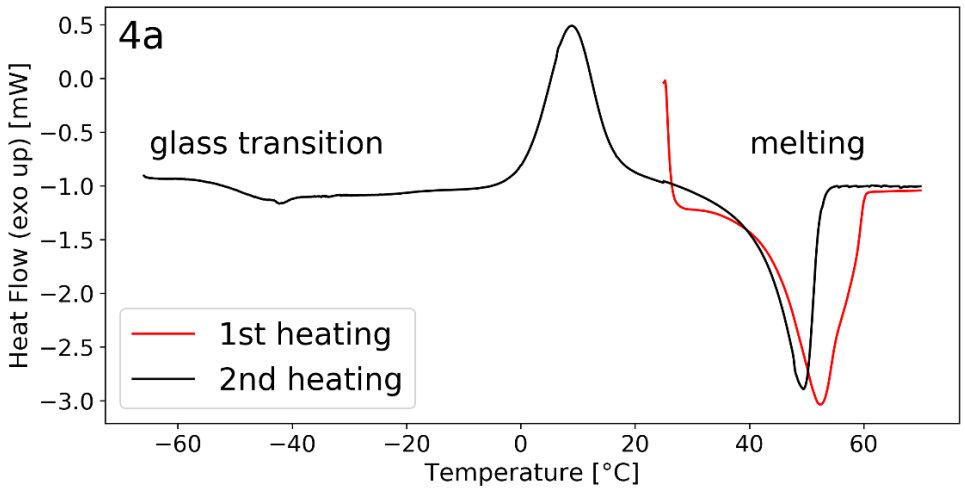

DSC curve of complex **4a** ($[P_{6,6,6,14}][Pt(PPy)Br_2]$).

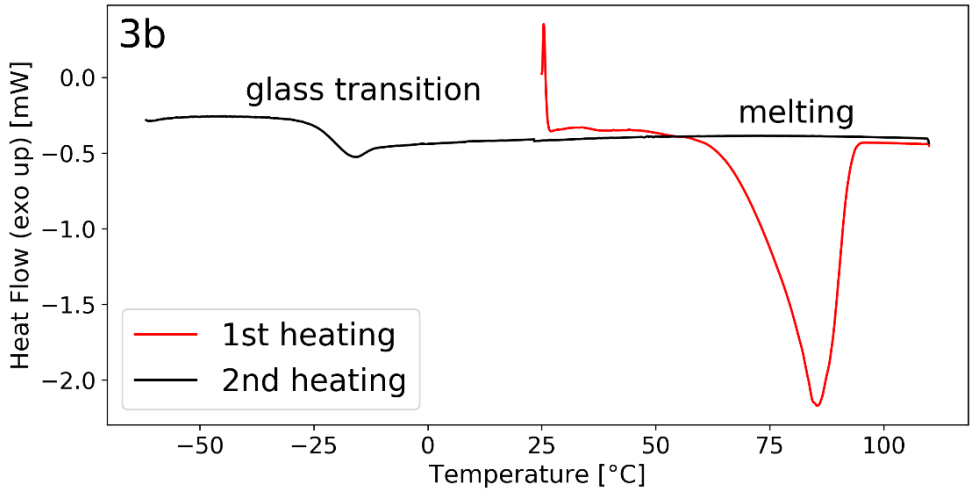

DSC curve of complex **3b** ($[BMIm][Pt(PPy)Cl_2]$).

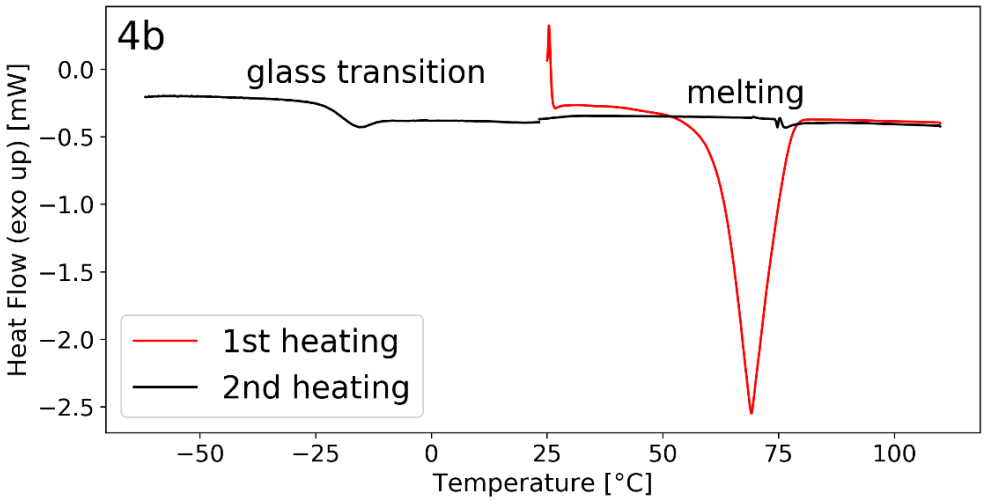

DSC curve of complex **4b** ($[BMIm][Pt(PPy)Br_2]$).

Appendix 9. Complex **3a** at different states under microscope with temperature control.

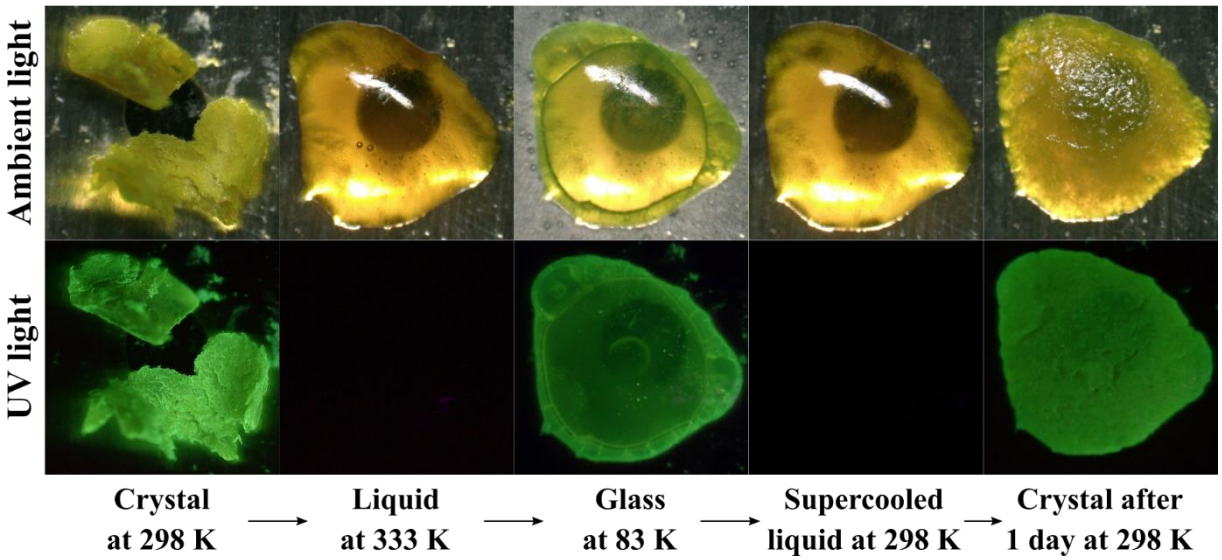

Appendix 10. Transparent luminescent film prepared from the complex **3a**.

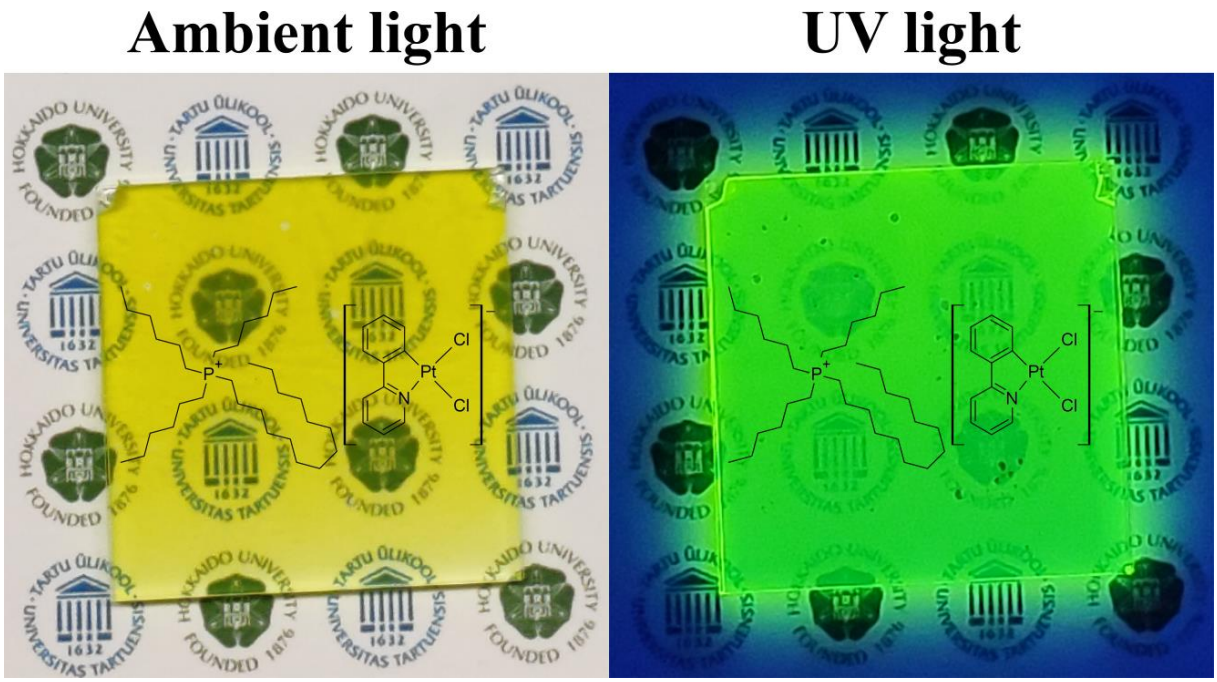

Non-exclusive license to reproduce thesis and make thesis public

Verner Sääsk (24.02.1998)

(*author's name*)

1. herewith grant the University of Tartu a free permit (non-exclusive license) to use my work,

Preparation of Luminescent Ionic Liquids Based on an Anionic Platinum(II) Complexes for Application in Optoelectronic Devices

(*title of thesis*)

supervised by Masaki Yoshida (PhD), Vladislav Ivaništšev (PhD) and Kaija Põhako-Esko (PhD)

(*supervisor's name*)

to reproduce it for the purpose of preservation and making available to the public, including for addition to the DSpace digital archives until expiry of the term of validity of the copyright, and

1.2. make available to the public via the university's web environment, including via the DSpace digital archives with the Creative Commons License CC BY NC ND 3.0, as of **03.06.2024** until expiry of the term of validity of the copyright,

2. I am aware of the fact that the author retains these rights.

3. This is to certify that granting the non-exclusive license does not infringe the intellectual property rights or rights arising from the Personal Data Protection Act.

Tartu, **26.05.2021**